

AD-780 266

HIGH-EFFICIENCY, SINGLE-FREQUENCY  
LASER AND MODULATION STUDY

Robert C. Ohlmann, et al

Lockheed Missiles and Space Company,  
Incorporated

Prepared for:

Office of Naval Research  
Advanced Research Projects Agency

30 September 1973

DISTRIBUTED BY:

**NTIS**

National Technical Information Service  
U. S. DEPARTMENT OF COMMERCE  
5285 Port Royal Road, Springfield Va. 22151

AD 780 266

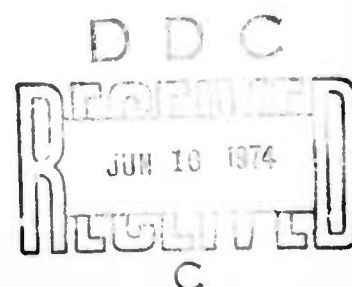
LMSC-D401776

HIGH-EFFICIENCY, SINGLE-FREQUENCY  
LASER AND MODULATOR STUDY

Third Semiannual Technical Report

N-JY-71-2

30 September 1973



R. C. Ohlmann, K. K. Chow, J. J. Younger, W. B. Leonard,  
D. G. Peterson, and J. Kannelaud

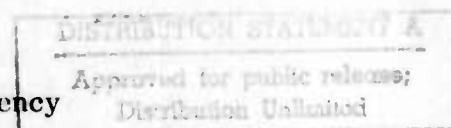
ARPA Order No. 306  
Expiration Date: 30 March 1974  
Amount: \$399,684

Contract No. N00014-71-C-0049  
Program Code 421  
Effective Date of Contract: 1 September 1970

Scientific Officer: Director, Physics Programs  
Physical Sciences Division  
Office of Naval Research, Arlington, Va. 22217

Principal Investigator: R. C. Ohlmann (415) 493-4411, Ext. 45275

Sponsored by  
Advanced Research Projects Agency



The views and conclusions contained in this document are those of the authors and should not be interpreted as necessarily representing the official policies, either expressed or implied, of the Advanced Research Projects Agency of the U.S. Government.

Lockheed Palo Alto Research Laboratory  
LOCKHEED MISSILES & SPACE COMPANY, INC.  
A Subsidiary of Lockheed Aircraft Corporation  
Palo Alto, California 94304

## CONTENTS

Section		Page
	ILLUSTRATIONS	iii
1	INTRODUCTION	1-1
2	SYSTEM DESIGN	2-1
	2.1 Modulation Formats and Bandwidth Considerations	2-1
	2.2 Quadriphase-Shift-Keying Digital Modulation	2-2
	2.3 FM Analog-Modulation	2-7
3	CRITICAL COMPONENTS AND SYSTEM IMPLEMENTATION	3-1
	3.1 The Optical Modulator	3-1
	3.2 Photodetectors	3-3
	3.3 PN Signal Generator and Biphase Modulators/ Demodulators	3-4
	3.4 The Voltage-Controlled Oscillator	3-10
	3.5 The Wideband FM Discriminator	3-12
	3.6 System Implementation	3-16
4	SYSTEM TESTS	4-1
	4.1 QPSK Digital Modulation Results	4-1
	4.2 FM-Analog Modulation Results	4-5
5	CONCLUSIONS AND FUTURE PLANS	5-1
6	REFERENCES	6-1

## ILLUSTRATIONS

Figure		Page
2-1	Block Diagram Showing Various Subsystems and Modulation Formats Used in the Laboratory Communication System Demodulation Demonstration	2-3
2-2	2-Gbits/sec Laboratory Laser Communication System: Optical Subsystem and Transmitter Electronics	2-4
2-3	2-Gbits/sec Laboratory Laser Communication System: Receiver Electronics	2-5
2-4	Diagram Illustration: the FM Subsystem and the Combination of FM Analog and QPSK Digital Signals	2-8
2-5	The FM Demodulation System	2-10
3-1	Modulation Index Versus Frequency for 7.5-mm-Length LiNbO <sub>3</sub> Crystal With rf Power in Reverse Direction	3-2
3-2	Modulation Index Versus Frequency for 7.5-mm-Length LiNbO <sub>3</sub> Crystal With rf Power in Forward Direction	3-2
3-3	Relative Optical Sideband Power as a Function of Modulation Frequency at Low-Drive Power Levels	3-3
3-4	Relative Frequency Response of the Varian Static Cross-Field Photomultiplier Tube	3-4
3-5	Block Diagram of a 500-Mbits/sec Word Generator	3-5
3-6	Use of Balanced Diode Modulator for Biphasic Modulation of rf Subcarrier	3-6
3-7	Demodulator Waveforms	3-9
3-8	Static Tuning Characteristics of the First Voltage-Controlled Oscillator, With Center Frequency of 3.5 GHz	3-11
3-9	Static Tuning Characteristics of the Second Voltage-Controlled Oscillator, With Center Frequency of 3.4 GHz	3-13
3-10	The Wideband FM Discriminator	3-14
3-11	Transmitter of 2-Gbits/sec Laboratory Optical Communication System	3-17
3-12	Receiver of 2-Gbits/sec Laboratory Optical Communication System	3-19

Figure		Page
4-1	Sampling Scope Display of Four 500-Mbits/sec Streams Transmitted Through the Laser Link	4-1
4-2	Waveforms of Two 500-Mbits/sec Streams on 2.5-GHz Subcarrier Frequency With Simultaneous 1-Gbit/sec Digital Signal on 3.5-GHz Subcarrier	4-2
4-3	Waveforms of Two 500-Mbits/sec Streams on 3.5-GHz Subcarrier Frequency With Simultaneous 1-Gbit/sec Digital Signal on 2.5-GHz Subcarrier	4-3

Section 1  
INTRODUCTION

The work described in this report is the final year's effort of a three-year program to study wide bandwidth laser communications at  $1.06\text{-}\mu\text{m}$  wavelengths. Earlier efforts of this program (during the first two years) were directed to studying the means to produce a high-efficiency, single-frequency neodymium doped yttrium aluminum garnet (Nd:YAG) laser operating at  $1.06\text{ }\mu\text{m}$ , and to produce high-efficiency, octave-bandwidth, microwave light modulators for this wavelength (Refs. 1 and 2). In addition, a study was also made of laser communication configurations that were suitable for very high data rates. The overall objective of this year's program, then, is to apply the results of these earlier studies to assemble a laboratory communication system that uses the entire modulation bandwidth available. In particular, the final result of this program is to be a laboratory demonstration of a laser-communication system having a bandwidth of 2 GHz.

The detailed objectives of this study program are as follows:

- Design a laboratory communication system, using  $1.06\text{-}\mu\text{m}$  radiation from a Nd:YAG laser and having a system bandwidth of 2 to 4 GHz
- Assess the state-of-the-art of high-frequency photodetectors, with emphasis on a cross-field photomultiplier tube (PMT), that offer good frequency and spectral response and are suitable as the receiver elements of this communication demonstration
- Define and design any necessary microwave, digital-modulation, and frequency-modulation subsystems for the communication system
- Assemble and operate the various subsystems
- Demonstrate and evaluate the system performance in a laboratory environment

During this first six-month period, much of the basic work has been accomplished: a laboratory communication system capable of transmitting data at a rate of 2 Gbits/sec has been assembled and tested, and work has been started on a 2-GHz system, of which one gigahertz will be used to transmit analog signal and the second gigahertz will be used to transmit a 1-Gbit/sec signal. A paper describing this initial work on the system test, entitled "Recent Advances in Ultrawideband Bandpass Optical Beam Modulators," has been submitted to the International Electron Devices Meeting to be held in Washington, D.C., in December.



## Section 2 SYSTEM DESIGN

### 2.1 MODULATION FORMATS AND BANDWIDTH CONSIDERATIONS

To transmit data at the high rates desired, microwave subcarrier modulation formats are chosen. That is, the information to be transmitted is first modulated onto a microwave carrier frequency (the subcarrier), which, in turn, is modulated onto the optical beam (the optical carrier). For a given modulation format, the data rate to be transmitted determines the required system bandwidth. Therefore, for this demonstration, the data rate has to be chosen so that the entire available microwave bandwidth of the optical modulator is used.

At the present moment, there is no one single data source that will occupy the octave band from 2 to 4 GHz. Therefore, to demonstrate the bandwidth capacity of this laboratory communication system, a convenient way must be devised. This is obtained by transmitting a number of signals filling that band; i.e., the demonstration can be accomplished by using several microwave subcarriers, each with its own sidebands, so as to fill up the entire modulation band of 2 GHz.

To carry out the demonstration in this fashion, two modulation formats have been chosen. One uses quadriphase-shift-keying (QPSK) of a microwave subcarrier to transmit digital signals; the other uses frequency modulation of a microwave subcarrier to transmit analog signals. In this way, both digital- and analog-signal transmission will be demonstrated. In fact, a combination of these two types of signals, filling the 2- to 4-GHz band, can be made to demonstrate simultaneous transmission of digital and analog signals. In the digital QPSK format, two streams of digital data at a rate of 0.5-Gbit/sec each are the most conveniently obtainable signals in a laboratory.\*

---

\*For a brief description of QPSK modulation, see subsection 2.2.



Such an arrangement gives a total data rate of 1 Gbit/sec and has sidebands occupying 1 GHz of bandwidth. For FM analog modulation, the modulation bandwidth is typically not limited by the signal sources; rather, it is limited by the devices that impress the modulation onto the subcarrier. One of these devices is usually a voltage-controlled oscillator (VCO) whose instantaneous frequency is a function of the input modulation voltage. In this case, a 1-GHz spectrum width is usually around the upper limit of available VCO's.

In this demonstration, therefore, we shall use either (1) two microwave subcarriers, each being QPSK-modulated at 1 Gbit/sec to get a total data rate of 2 Gbits/sec; or (2) two subcarriers, one QPSK-modulated to give 1 Gbit/sec and the other modulated by various FM signals to occupy a gigahertz of bandwidth. In this way, both types of modulation signals will be used and performance of the system will be investigated. Figure 2-1 is a block diagram showing the use of these various formats in this demonstration. The choice of subcarrier frequencies for these formats will be discussed in the following subsections.

## 2.2 QUADRI PHASE-SHIFT-KEYING DIGITAL MODULATION

Detailed block diagrams of this laboratory laser-communication system using QPSK modulation format to transmit a 2-Gbits/sec data stream is shown in Figs. 2-2 and 2-3. The optical subsystem, the digital modulation subsystems, and the modulation driver are shown in Fig. 2-2. The microwave receiver, which amplifies the output of the photodetector, and the subsequent digital demodulation subsystems are shown in Fig. 2-3. The optical subsystem is self-explanatory; the laser and the modulator were both developed under this contract in an earlier phase. The photodetector, however, is a commercial one, and there is yet no one photodetector that is suitable for our demonstration. This point will be elaborated in subsection 3.2.

In such a digital QPSK modulation subsystem, a cw microwave signal is used as a subcarrier. Modulation of the subcarrier by the digital data results in a change of the rf phase of the subcarrier. These are shown in detail in the phasor diagram presented in

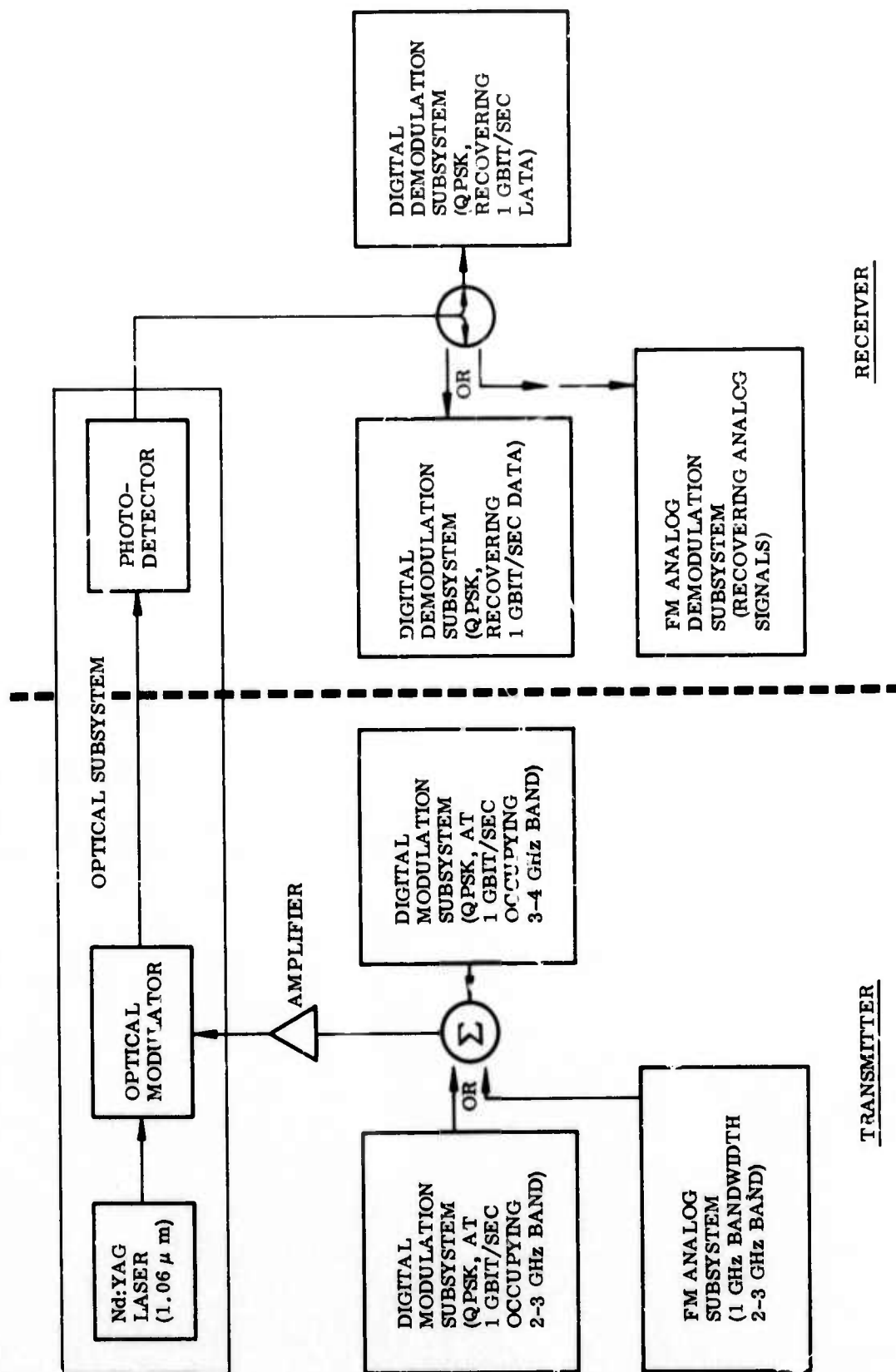


Fig. 2-1 Block Diagram Showing Various Subsystems and Modulation Formats Used in the Laboratory Communication System Demonstration

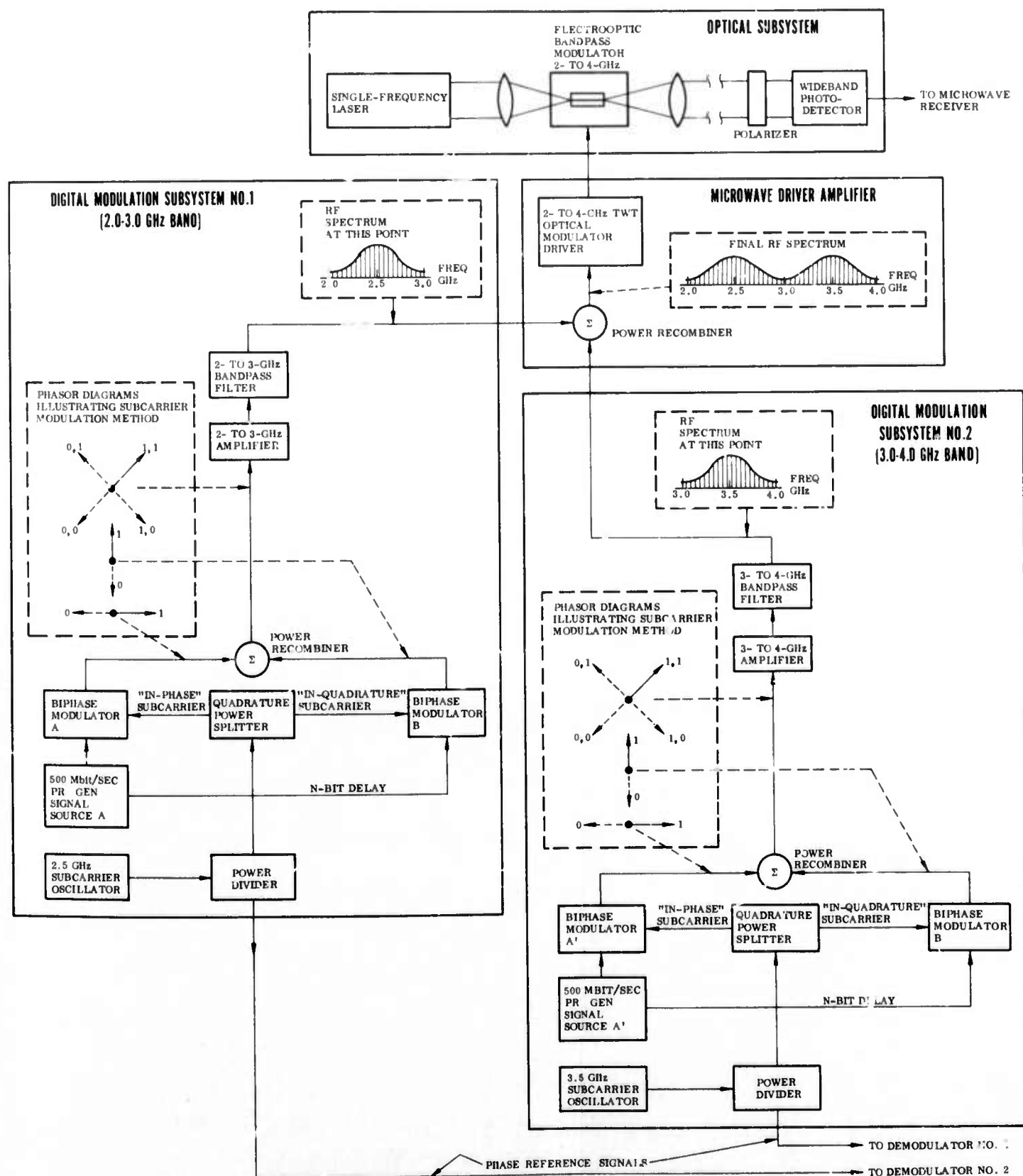


Fig. 2-2 2-Gbits/sec Laboratory Laser Communication System: Optical Subsystem and Transmitter Electronics

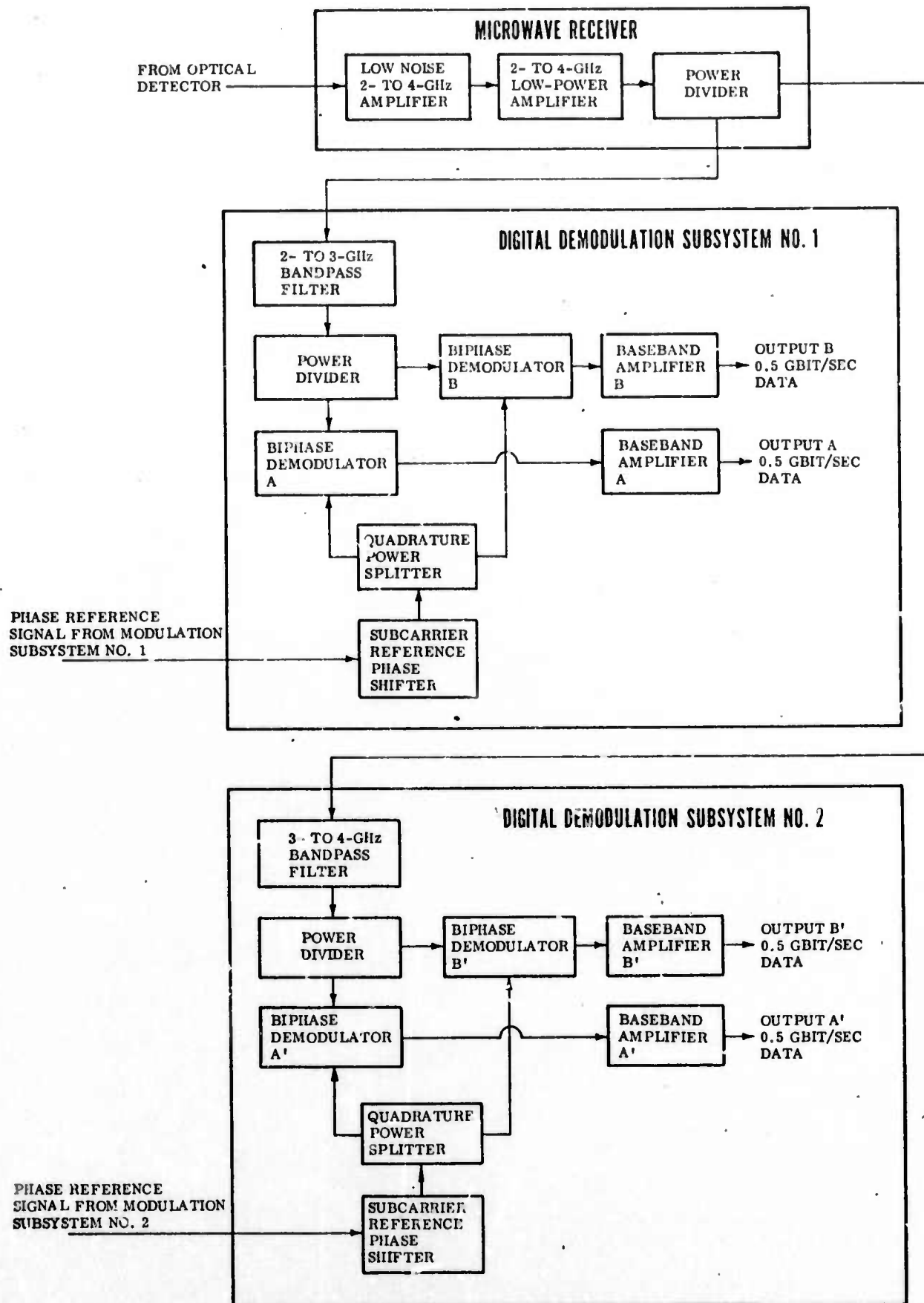
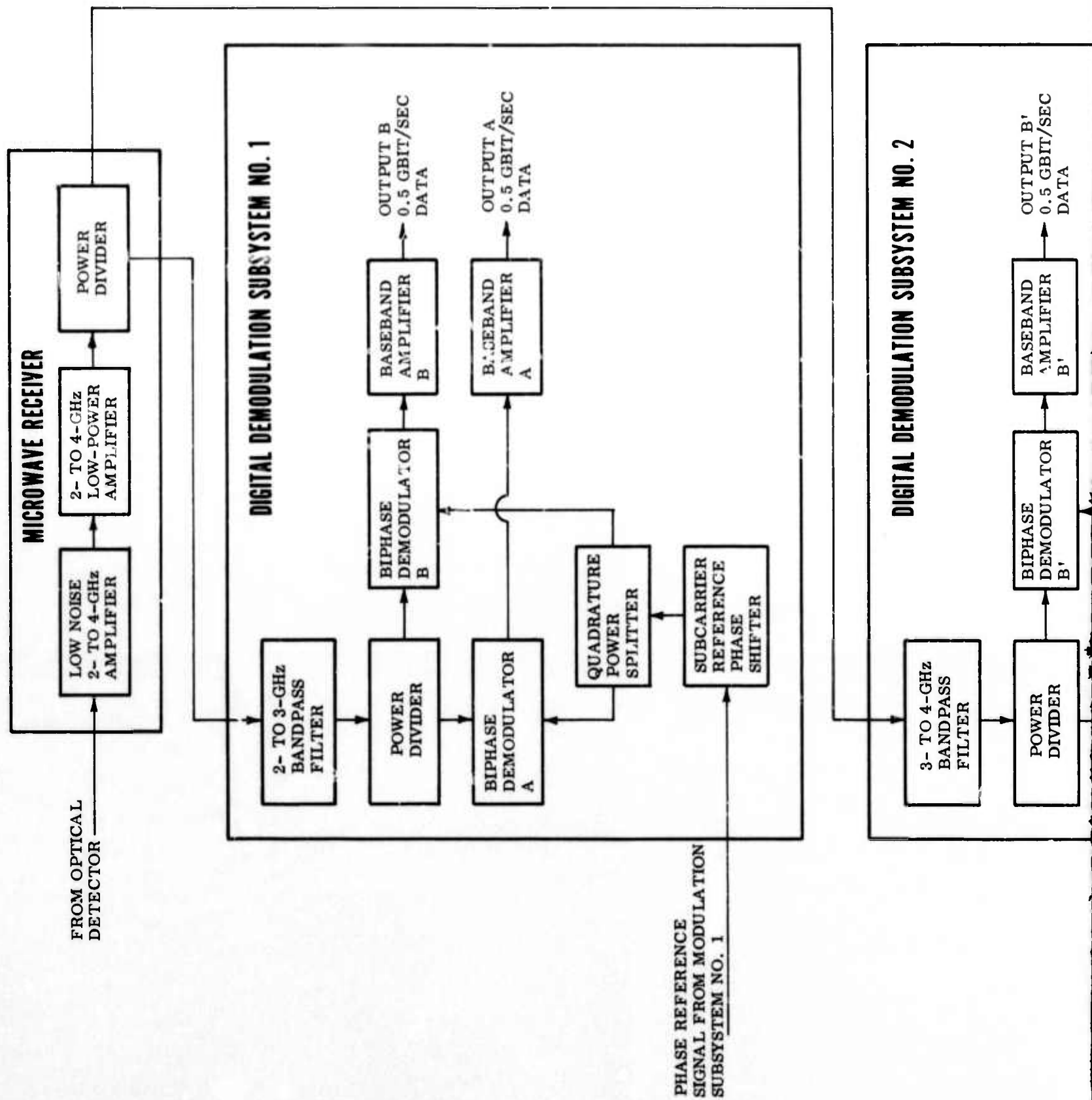


Fig. 2-3 2-Gbits/sec Laboratory Laser Communication System: Receiver Electronics

LMSC-D401776



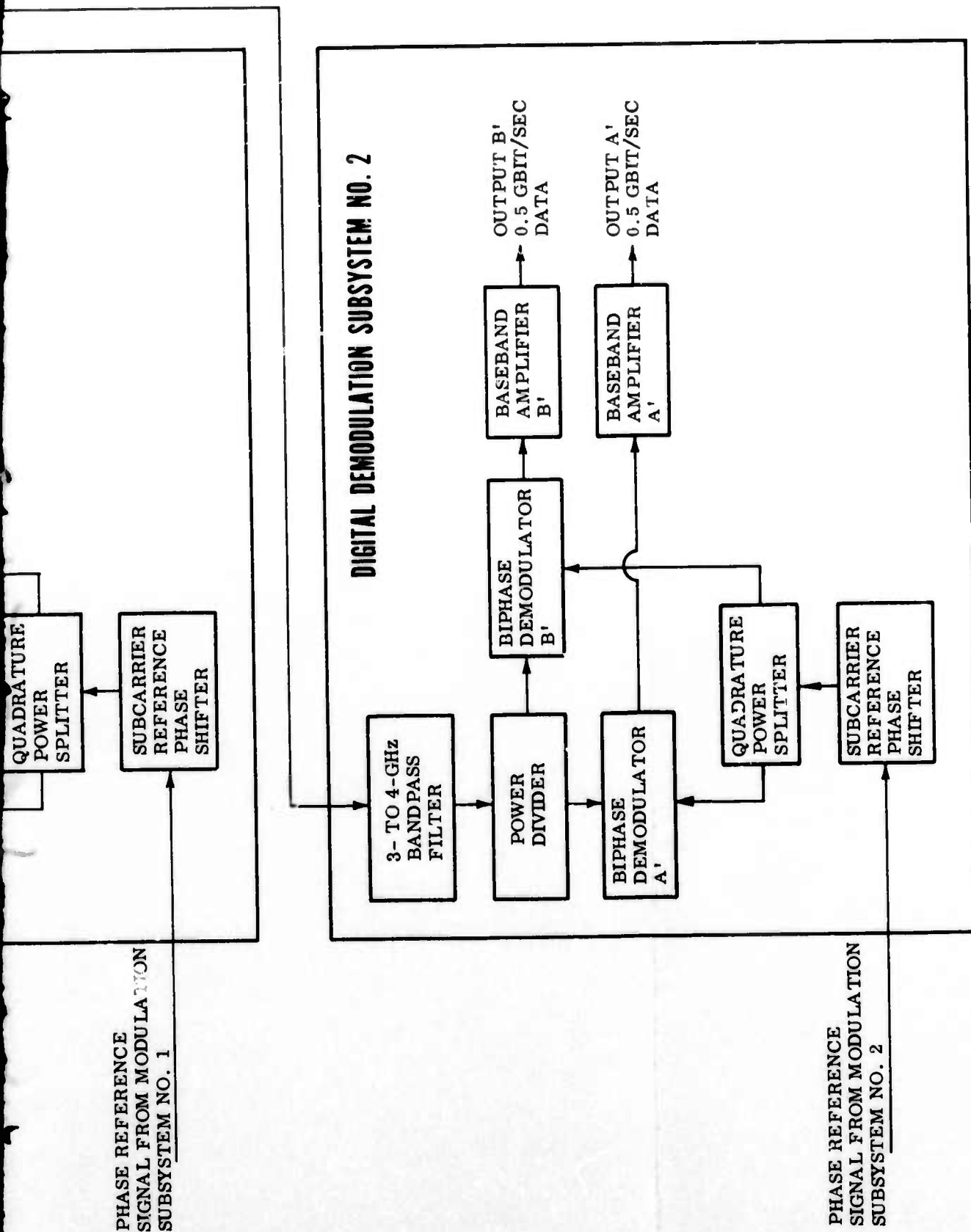


Fig. 2-3 2-Gbits/sec Laboratory Laser Communication System: Receiver Electronics

Fig. 2-2. Because of the required bandwidth considerations, as discussed in subsection 2.1, two subcarriers are chosen — one at 2.5 GHz, and the other at 3.5 GHz. Each subcarrier is split into two channels: one "in-phase" channel and one "in-quadrature" channel. Each of the channels is then biphase-shifted at a biphase modulator by an independent 500-Mbits/sec simulated data stream from a pseudo-random (PN) signal generator as shown in the associated phasor diagram in Fig. 2-2. That is, the phase of the microwave subcarrier of that channel is reversed at each change of state of the signal at the binary input terminal of the biphase modulator. Thus, if the modulating signal is a binary "1," the phase of that channel is undisturbed. If, on the other hand, the modulator signal is a binary "0," the phase of that channel is reversed (switched by 180 electrical degrees as shown dotted in the phasor diagram).

Since the two channels are already in quadrature, the two biphase modulators will give four possible quadrature phase relationships. Therefore, the combination of the two channels results in the final phasor relationship shown in Fig. 2-2 and gives a total data rate of 1 Gbit/sec for that subband.

At an input data rate of 1 Gbit/sec, the sideband power of QPSK modulation has first nulls at 500 MHz above and below the subcarrier frequency. Outside the first nulls, the power content is negligible. Therefore, for each subband, the center frequency of the subband is chosen as the subcarrier frequency (2.5 and 3.5 GHz as mentioned earlier), and a 1-GHz bandpass filter (2 to 3 GHz and 3 to 4 GHz) is used to reject the sideband power outside the first nulls. Combination of these two subbands gives a total data rate of 2 Gbits/sec. This is amplified by a 10-W traveling-wave tube (TWT) to drive the optical modulator.

In the photodetector, the optical carrier is detected to recover the microwave subcarriers and their sidebands which are then sent to the first amplifier in the receiver subsystem. After amplification, the microwave signal is divided into two halves as shown in Fig. 2-3. Each half is filtered to give one of the subbands which is then further divided into two channels. The signal in each channel, together with a strong



"in-phase" or "in-quadrature" reference, is directed to a biphase demodulator. In a communications system, the reference signals required are normally derived from the incoming signals. For the ease of this demonstration, however, the reference signals are taken from the transmitter directly by separate cables (hardwire references) to demonstrate the capacity of the laser communications system, without having to deal with the added complications of phased-locked loops, etc. for the derivation of the reference signals. These hardwire references are clearly indicated in Figs. 2-2 and 2-3.

The biphase demodulator performs synchronous demodulation of the received QPSK signal by comparing its phase with that of the reference signal. The output signal of the biphase modulator is filtered and amplified by a baseband amplifier to recover the 500 Mbits/sec digital data at each channel. This will be discussed in greater detail in subsection 3.3. Two 500-Mbits/sec streams are recovered for each subband; i. e., a total of 2 Gbits/sec data is recovered from both subbands.

It should be emphasized here that, although the 500-Mbits/sec PR signals for both channels in the subband are synchronous as used here in the demonstration, this system will accept synchronous data with only minor degradation. This has been demonstrated in an earlier experiment conducted at LMSC (Ref. 3).

### 2.3 FM ANALOG-MODULATION

For the transmission of analog signals, frequency modulation of a microwave sub-carrier is chosen. The block diagram for this particular form of modulation is shown in Fig. 2-4; the heart of the modulation subsystem is the voltage controlled oscillator (VCO). The VCO accepts amplified baseband analog signals (e. g., from local TV stations) and uses them to control a voltage-sensitive tuning element of the oscillator, typically a varactor diode. Thus, the instantaneous output frequency of the oscillator is proportional to the instantaneous voltage of the analog signal. For this experiment, several local TV channels, as well as an audio signal source which modulates a narrow band FM (NBFM) 400-MHz signal generator, are chosen so that the sidebands

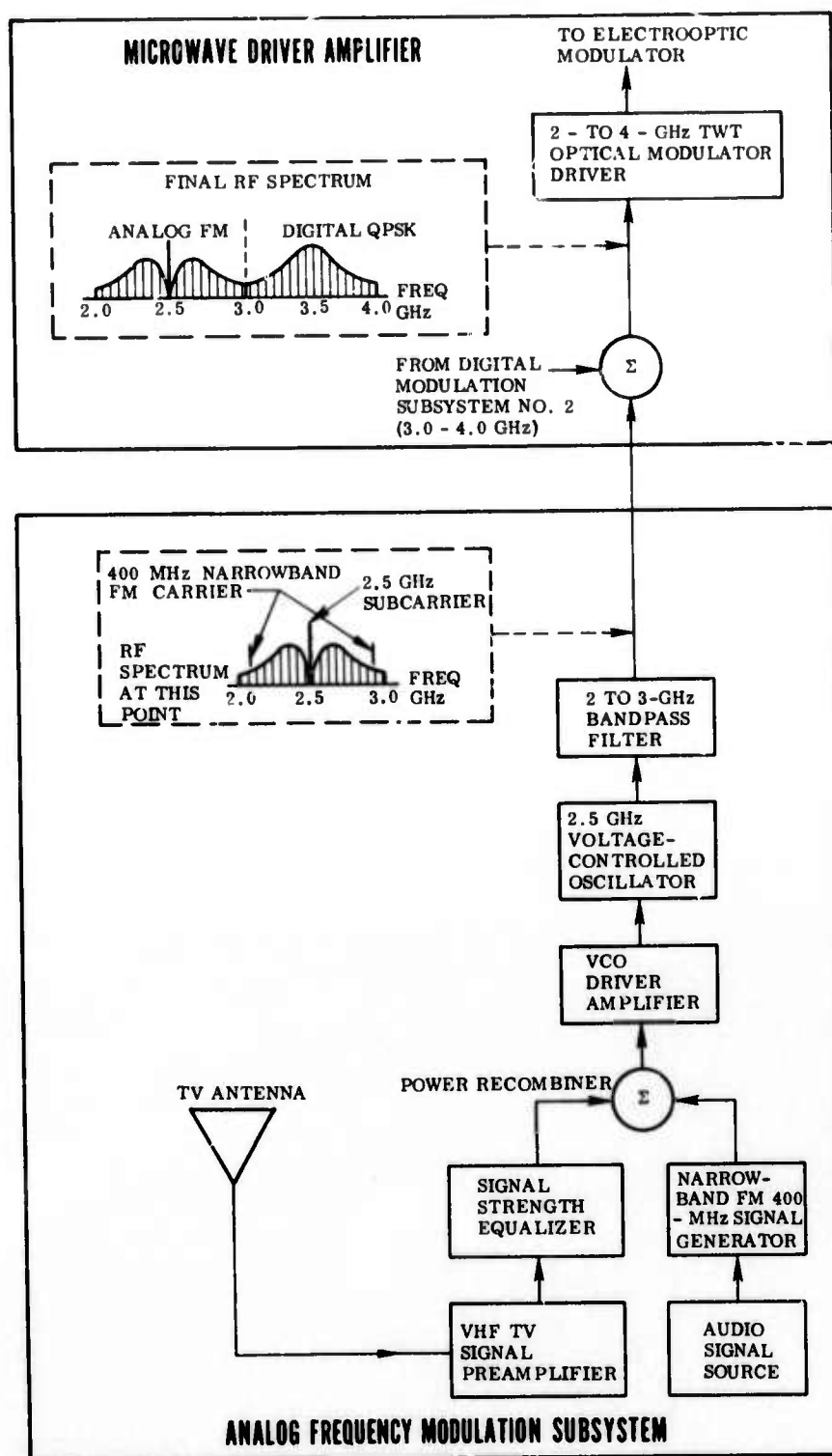


Fig. 2-4 Diagram Illustration: the FM Subsystem and the Combination of FM Analog and QPSK Digital Signals

of the VCO occupy practically the entire gigahertz band. TV signals and audio FM 400-MHz signals are combined, amplified, and used to control the frequency of the VCO. At the beginning of this experiment, the microwave subcarrier for the FM subband was chosen to be 3.5 GHz because it was believed that VCOs having 400 MHz of linear tuning range could be obtained more easily at a 3.5-GHz center-frequency. However, experience gained during this program showed that such was not necessarily the case. In addition, the poor frequency response of photodetectors at the high-frequency end (2- to 4-GHz band), coupled with the requirement that analog TV signals require rather high signal-to-noise (S/N) ratio to attain good reception and presentable pictures, changed our earlier thoughts about the choice of this subcarrier frequency. As a result, 2.5 GHz has been chosen as the subcarrier frequency for the analog signals, and a demonstration experiment will be performed in the next half-year using this subcarrier frequency.

In this experiment, the TV signals and the 400-MHz NBFM signal are combined and amplified to drive the VCO. From the VCO, the signal is passed through a 2- to 3-GHz bandpass filter to eliminate undesirable sidebands and spurious signals. The rf spectrum at that point (after the bandpass filter) is then as shown in Fig. 2-4. This signal is sent to the power recombiner to replace the lower subband of the digital QPSK signals (the 2- to 3-GHz subband) as shown in Fig. 2-1. After combination with the upper subband containing the other digital QPSK signals (the 3- to 4-GHz subband), the combined signal is sent to the traveling wave tube (as shown in Fig. 2-2) for the modulation of the optical signal.

The demodulation system for the FM subband is rather simple as shown in Fig. 2-5. The received signal from the photodetector is again split into two halves; one of them goes to the 3.5-GHz subcarrier digital demodulation circuit as before, while the other is directed to the FM demodulation subsystem as shown in Fig. 2-5. This signal is filtered by a 2- to 3-GHz bandpass filter and sent through a wideband FM discriminator, and then amplified by a baseband amplifier to recover the TV signals and the 400-MHz NBFM signal.

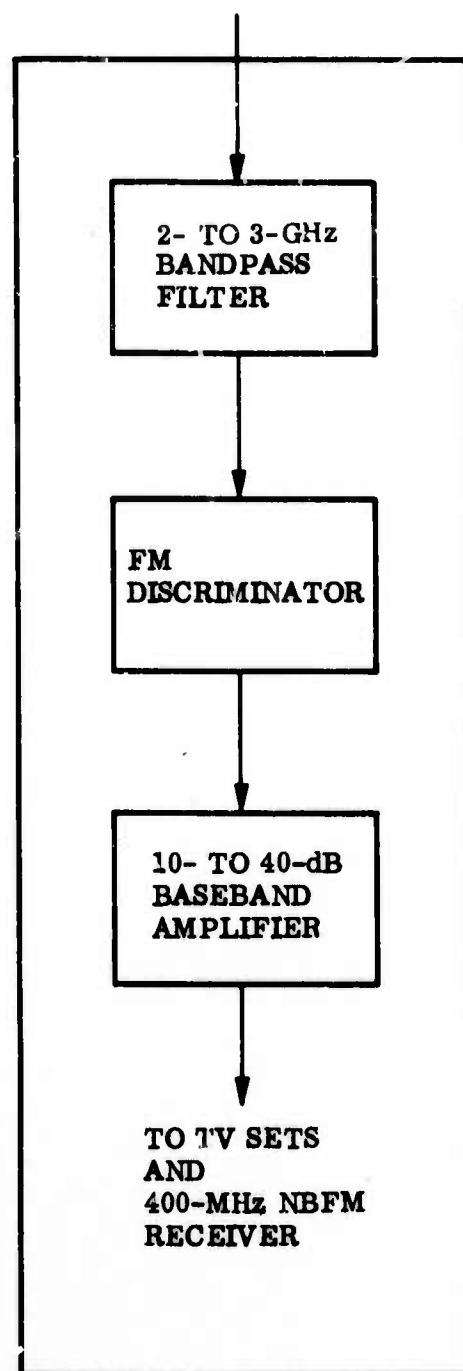


Fig. 2-5 The FM Demodulation System

### Section 3

## CRITICAL COMPONENTS AND SYSTEM IMPLEMENTATION

### 3.1 THE OPTICAL MODULATOR

During these first six months, additional effort was spent in improving the 2- to 4-GHz electrooptic modulator, since this modulator is the heart of this demonstration. Much improvement has been obtained, as reported in the following paragraphs.

After the approaches were initiated last year, the "reverse-flow" mode of operation was investigated further. This is the mode in which the rf drive power for the optical modulator flows through the circuit in such a way that the electrooptic modulating crystal is at the input digit. Previous work had rendered rather unsatisfactory results (Ref. 2) in terms of frequency response and modulation efficiency (modulation index/unit drive power/unit modulation bandwidth). During the past few months, through painstaking tuning and matching procedures, improved performance over the "forward-flow" mode was obtained, as shown in Fig. 3-1. At a 6-W input drive level, an average of 60-percent modulation index across a 3-dB bandwidth of 2.07 to 4.00 GHz is obtained. This is a definite improvement over the "forward-flow" mode obtained last year, shown in Fig. 3-2 as a comparison, for which approximately 62-percent average modulation index was obtained at about a 10-W drive level.

It appears from Fig. 3-1 that the modulator was tuned to a higher passband than the desired 2 to 4 GHz, because the low-frequency end showed a sharp drop while the high-frequency end showed uniform response to the band-edge. Therefore, additional turning effort was applied to move the passband lower. This was met with some success: Fig. 3-3 shows the relative optical sideband power as a function of modulation frequency at low-drive power levels. At these drive levels and using this particular method of measurement, the modulation index  $m$  is approximately proportional

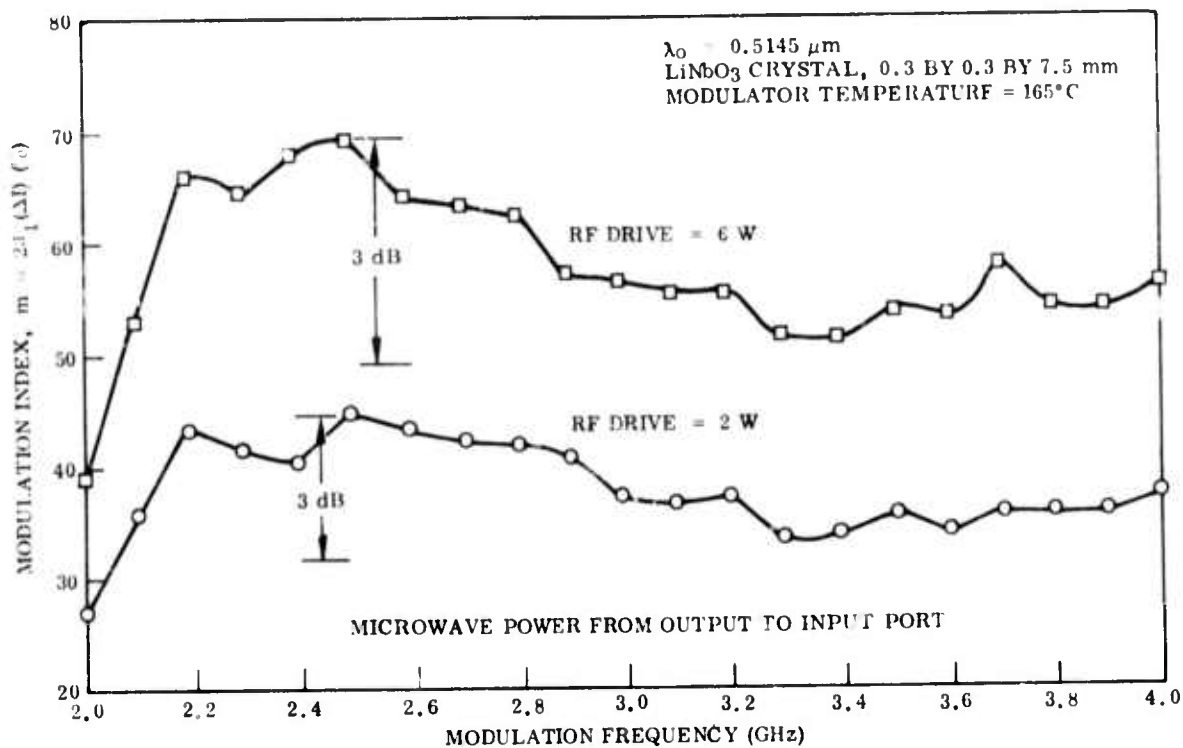


Fig. 3-1 Modulation Index Versus Frequency for 7.5-mm-Length  $\text{LiNbO}_3$  Crystal With rf Power in Reverse Direction

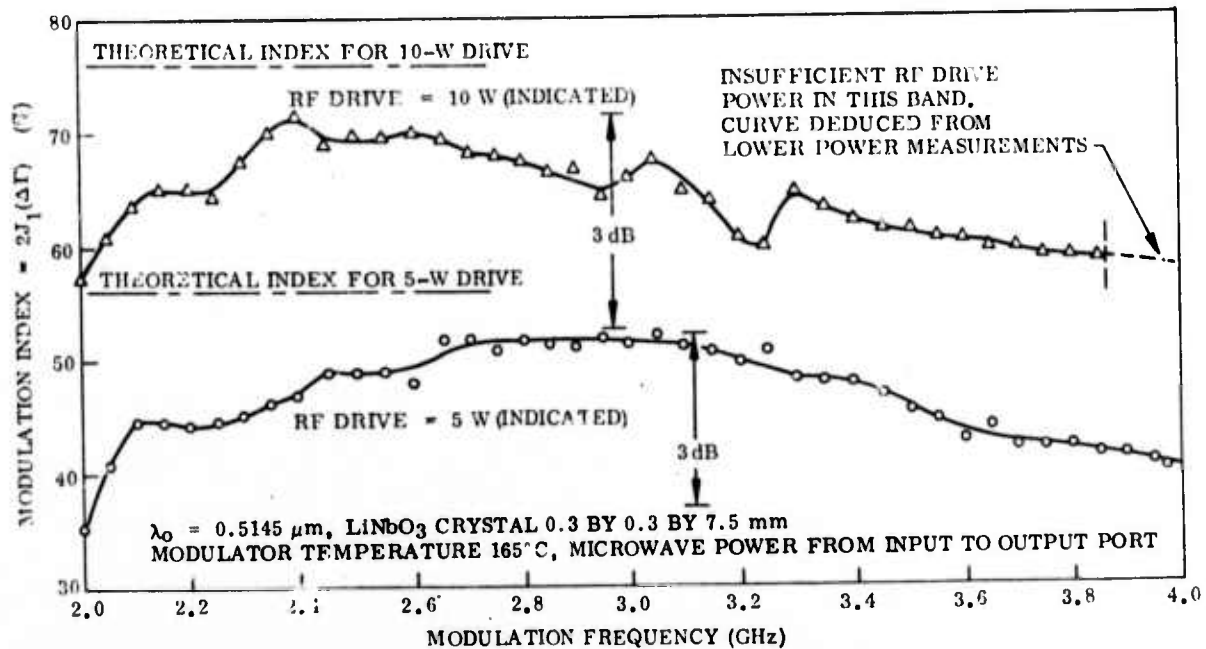


Fig. 3-2 Modulation Index Versus Frequency for 7.5-mm-Length  $\text{LiNbO}_3$  Crystal With rf Power in Forward Direction. (Results were obtained last year and are included here for purpose of comparison)

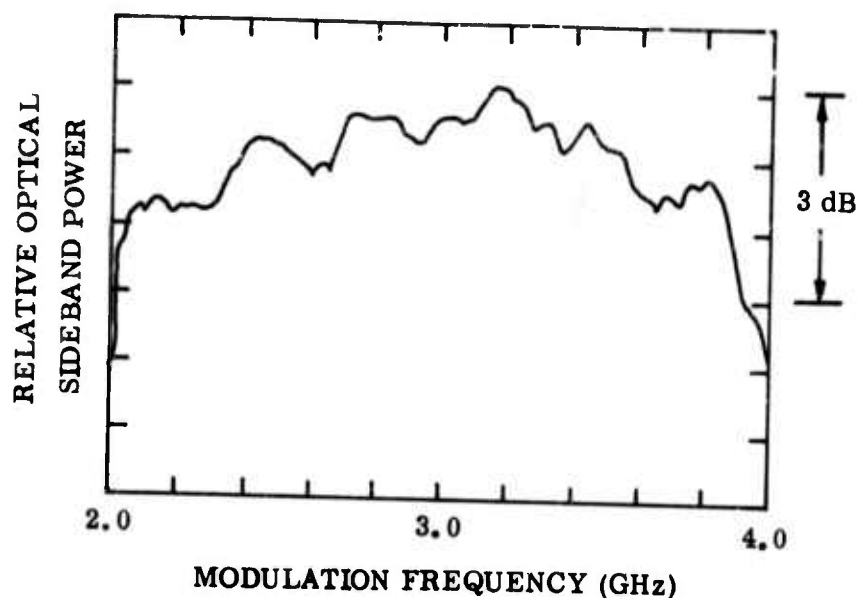


Fig. 3-3 Relative Optical Sideband Power as a Function of Modulation Frequency at Low-Drive Power Levels

to the square of the sideband power. Thus, the 3-dB level is about half-way down from the peak, as indicated in Fig. 3-3, and no increase in bandwidth over that shown in Fig. 3-1 is observed. Actual measurement of modulation index near the peak response showed that 80-percent modulation index for  $0.5145 \mu\text{m}$  was obtainable at 8.3 W of rf drive power; this value also agrees well with that scaled up from Fig. 3-1. However, the peak response is now considerably broader and more centered in the passband than that shown in Fig. 3-1. In this respect, improvement in modular performance has been achieved.

### 3.2 PHOTODETECTORS

For the laboratory demonstration, an experimental static cross-field photomultiplier tube (CFPM1) having a III-V compound (InGaAsP) photocathode was ordered from Varian Associates. This order was initiated in the belief that good quantum efficiency,



low noise figure, and good frequency-response at 4 GHz could all be obtained under a "best-effort" arrangement. Unfortunately, the CFPMT received falls short of our expectations: quantum efficiency is less than 1 percent, frequency response above 3.5 GHz is poor and, worst of all, there is a spurious resonance at about 2.5 GHz, which is also one of the subcarrier frequencies. The frequency response of the CFPMT is shown in Fig. 3-4. Therefore, another CFPMT, which did not appear to have this strong resonance, was used for the detection of 2-Gbits/sec optical data transmission.

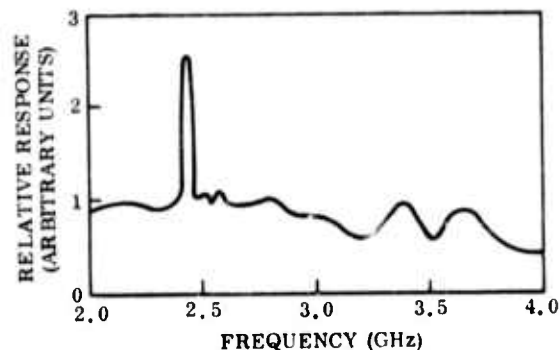


Fig. 3-4 Relative Frequency Response of the Varian Static Cross-Field Photomultiplier Tube

### 3.3 PN SIGNAL GENERATOR AND BIPHASE MODULATORS/DEMODULATORS

In the digital modulation subsystem, two important subassemblies are required. These are the 500-Mbits/sec pseudorandom (PR) signal generators and the balanced biphase modulators.

A convenient way of producing a 500-Mbits/sec PR signal stream is to combine the output of a 250-Mbits/sec maximal-length PR signal generator. Such a generator produces a  $2^{11} - 1$  ( $= 12047$ ) bit binary word. Since maximal-length signals separated by more than 1 bit are uncorrelated, two remote taps from this PR generator can be used to produce

a  $2^{12} - 2$  (= 4094) bit word at 500 Mbits/sec by interleaving the signals at the taps. This combination may be done by means of a MOD-2 circuit.

The 500-Mbits/sec PR generators of this kind have been fabricated at LMSC through our Independent Research efforts. The 2047-bit-length PR signals were produced by using an 11-stage feedback shift register. Good response time was obtained by using a hybrid integrated circuit MOD-2 adder and buffers as shown in Fig. 3-5. The rise times of the signals from the 250-Mbits/sec PR generator were improved by the dual hybrid buffer. The hybrid MOD-2 adder constructed the 500-Mbits/sec word, and the final hybrid buffer squared up the rise and fall times. Laboratory measurement shows that the rise and fall times are all subnanosecond and there is no incomplete bit. In the laboratory demonstration, the output from such a 500-Mbits/sec generator is used to modulate either a 2.5-GHz or a 3.5-GHz subcarrier by means of a biphase modulator.

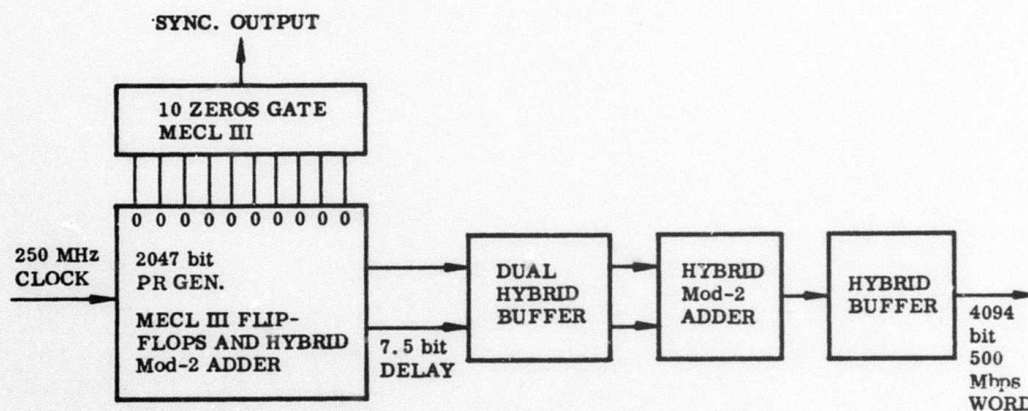


Fig. 3-5 Block Diagram of a 500-Mbits/sec Word Generator

The biphase modulator, using diode switches in a balanced construction, is used in this experiment and is shown in Fig. 3-6. Functionally, the modulator shown in Fig. 3-6 consists of two broadband transformers, each accurately center-tapped, and a ring of four fast-response diodes. The diodes are of Schottky type; the transformers can

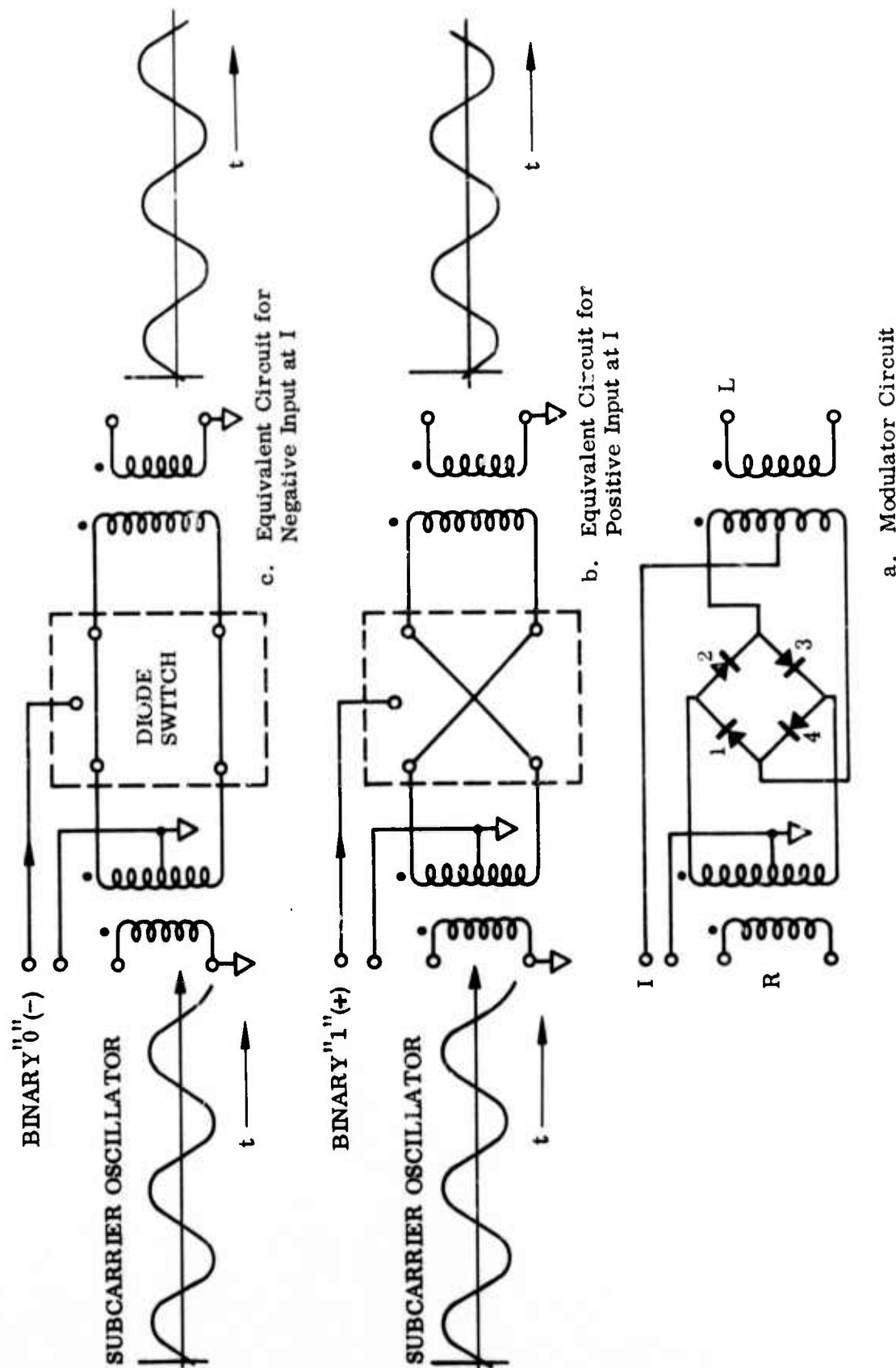


Fig. 3-6 Use of Balanced Diode Modulator for Biphase Modulation of rf Subcarrier

be either lumped-circuit devices or coaxial or waveguide structures. The modulators employed here have octave bandwidths for ports R and L, and a 0- to 1-GHz bandwidth for port I. The balanced structure minimizes undesired coupling between the various ports.

When used as a modulator, the cw microwave subcarrier is applied to port R; the non-return to zero (NRZ) digital control signal is applied to port I; and the modulated output signal is taken from port L. The amplitude of the sinusoidal subcarrier at port R is made to be much smaller than the control voltage at port I. The control voltage is made to be negative at the upper terminal of port I to represent a binary bit "0" and positive to represent a binary bit "1." When the control voltage is negative, diodes 2 and 4 are made to conduct fully and therefore appear as low impedances, whereas diodes 1 and 3 are back-biased and appear as high impedances. The equivalent circuit for this condition is shown in Fig. 3-6c, where the microwave subcarrier at the input port is transferred to the output port with the same phase.

To represent a binary bit "1," the upper terminal of port I is made positive, thereby causing diodes 1 and 3 to conduct and diodes 2 and 4 to be back-biased. The equivalent circuit is shown in Fig. 3-6b. The phase of the microwave subcarrier at the output port is then reversed from that at the input port. Therefore, the device operates as a biphase modulator. When a 500-Mbits/sec digital signal modulates a 2500-MHz subcarrier, five subcarrier cycles per data bit occur.

The foregoing discussion may be regarded as the modulation of the "in-phase" component of the microwave subcarrier. Modulation of the "in-quadrature" portion of the subcarrier is accomplished in the same way. A delayed output (by N-bits) of the 500-Mbits/sec generator is directed to port I while the "in-quadrature" subcarrier is directed to port R of the other biphase modulator (biphase modulator B in Fig. 2-2). The two modulated subcarriers are then recombined at the power combiner to give a quadriphase-shift-keyed 2.5-GHz subcarrier modulated at a rate of 1 Gbits/sec. Quadriphase shift-keying modulation of the 3.5-GHz subcarrier is accomplished in the same fashion.

In the demodulator (Fig. 2-3), the signal is again split into two streams, each to be demodulated by a biphase demodulator, which is identical in construction to that of the modulator. When the device is used as a demodulator, a coherent reference cw microwave signal is applied to either port R or port L, and the signal to be demodulated is applied to the remaining port of R or L. "Demodulated baseband signal" is taken from port I. In this application, the reference signal is made much larger than the signal being demodulated. For simplicity, the reference signal for each subband is taken directly from the appropriate subcarrier oscillator through a precision phase shifter to ensure proper phase relationship between the reference and the received signals. In contrast to operation of the device as a modulator, switching of the diodes takes place twice during each cycle of the microwave reference signal rather than only at the data rate.

When the reference at port R is positive, diodes 2 and 3 conduct, whereas diodes 1 and 4 are back-biased. This has the effect of placing the top of the center-tapped winding of port L transformer at virtual ground and open-circuiting the bottom of that transformer. The effect is to cause the voltage of port L to appear inverted at port I. When the reference at port R is negative, the inversion occurs.

Figure 3-7 shows the waveforms obtained when the device is used as a demodulator. The reference signal at port R is shown at Fig. 3-7a, with a typical biphase input signal shown at Fig. 3-7b. The demodulated output at Fig. 3-7c is seen to contain the data (0010) and harmonics of the subcarrier. The latter are removed by filtering and gives a more readily recognizable baseband signal of (0010) as shown in Fig. 3-7d.

It is instructive to follow through the response of the demodulator when it is presented with a biphase-modulated quadrature subcarrier. This is indicated in Fig. 3-7e, where a subcarrier with the modulation of 0100 is shown, and in Fig. 3-7f, where the output response for that signal is shown. No data components are present in this output; the output is only harmonics of the subcarrier, and they are filtered out before use.



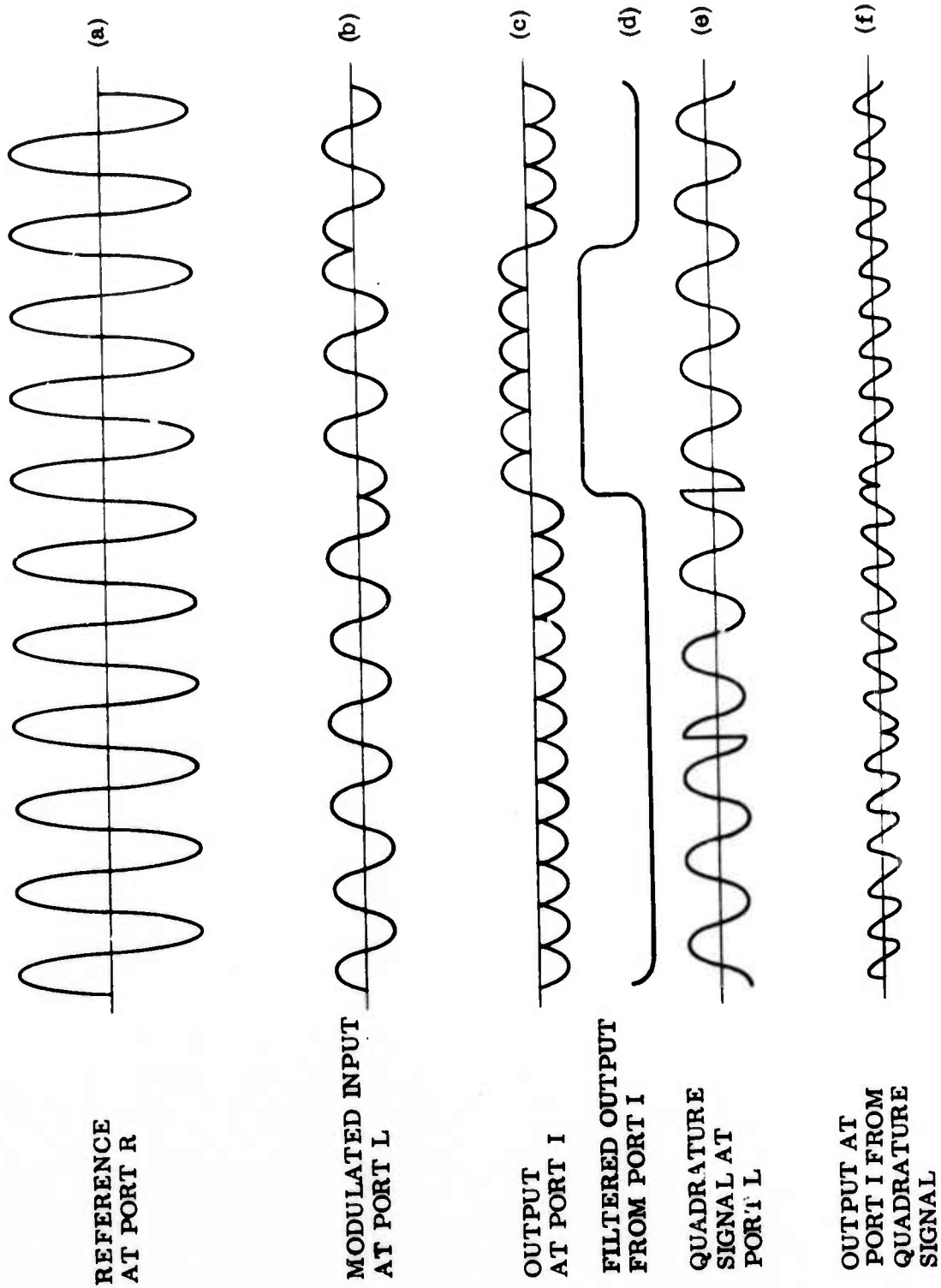


Fig. 3-7 Demodulator Waveforms

Because the reference signal is large, the device acts as a linear element with respect to modulated signals as port L. The waveforms of Fig. 3-7 indicate what occurs when the signal at port L is a quadriphase signal, such as the sum of the signals shown in Fig. 3-7b and 3-7e. In that case, the output would be the sum of the waveforms shown in Fig. 3-7c and 3-7f; i.e., the only signal remaining after filtering would be that of the modulation (0010) on the in-phase subcarrier. A second demodulator using a quadrature reference with the same modulated signal applied to its port L would produce only 0100 as its filtered output. That is, the two 500-Mbits/sec channels in the QPSK system are independent.

### 3.4 THE VOLTAGE-CONTROLLED OSCILLATOR

The key component for frequency-modulated transmission of analog signals is a voltage-controlled oscillator (VCO). This is a solid-state device using transistors for the amplifying elements and voltage-tunable capacitors (varactor diodes) as the voltage-controlled tuning element. Figure 3-8 is a typical static voltage tuning curve of such a device, and shows that, over octave bandwidths, these devices are rather nonlinear. However, if the modulating voltage swing is kept small, it is possible to produce a relatively linear response. This is important for the effective transmission of broadband signals. Otherwise, the various parts of the modulating spectrum mix together to produce intermodulation distortion. For a required bandwidth, therefore, it is desirable to keep the subcarrier frequency as high as possible to reduce the percentage bandwidth. In this way the linearity problem of the VCO can be minimized.

For this reason, it was decided at the beginning of this year to use the 3.5-GHz subcarrier for the FM portion of this demonstration. A VCO having a center frequency of 3.5 GHz was ordered from Watkins-Johnson Company, the tuning characteristic of which has been shown in Fig. 3-8. The linearity over a small deviation frequency (e.g., 36 MHz) is reasonable; unfortunately, the drive voltage requirement is too high. For instance, for a deviation of 36 MHz, a peak-to-peak voltage swing of 16 V from a UHF analog amplifier is required. This corresponds to 0.64 W output from the UHF amplifier; such power levels are just at the saturation limit of the present state-of-art wide-band UHF amplifiers. While the desired amplifier power can be made available, saturation effects occurring within the amplifier produce intermodulation between various analog signals and give rather undesirable results.



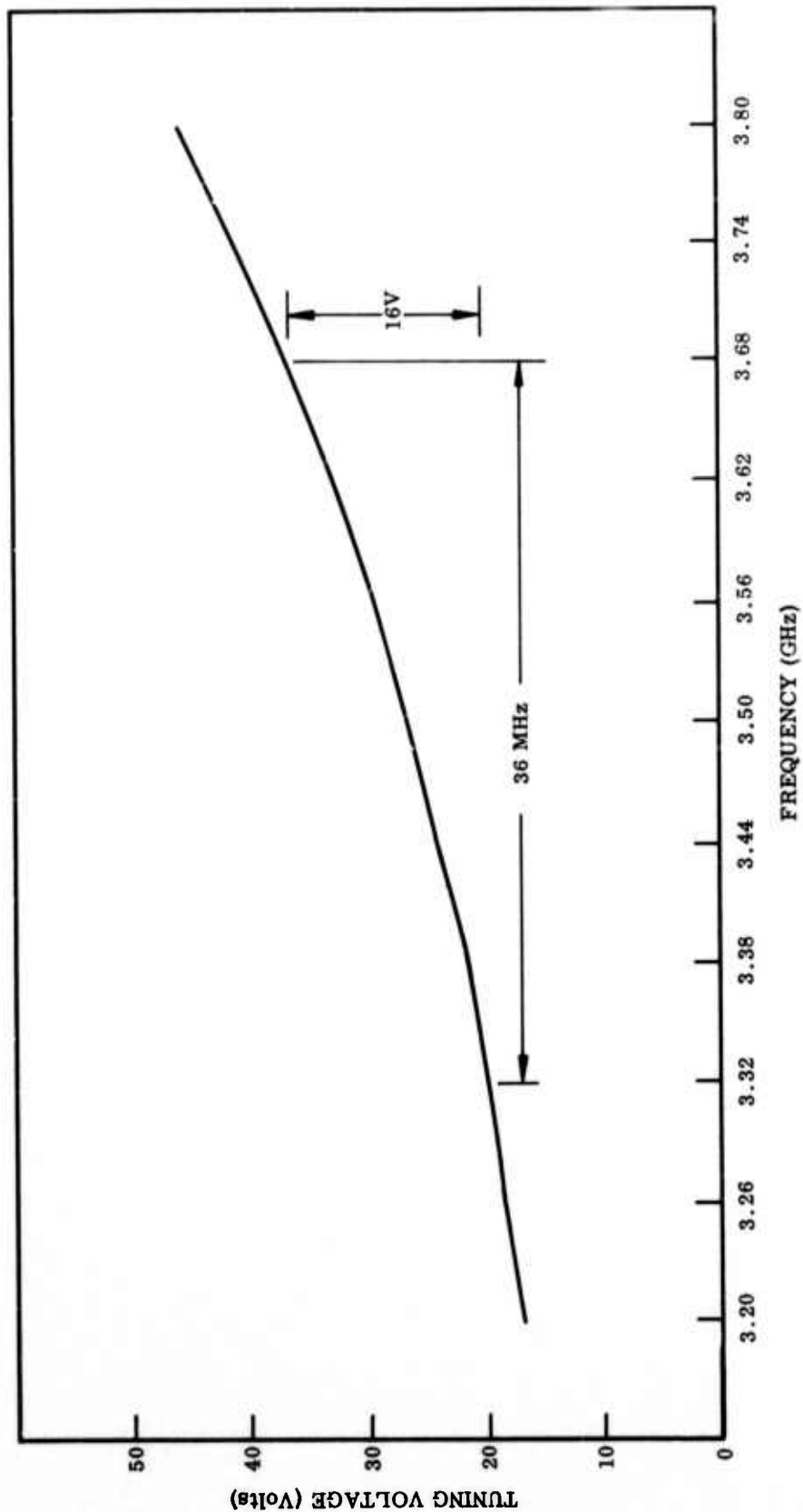


Fig. 3-8 Static Tuning Characteristics of the First Voltage-Controlled Oscillator, With Center Frequency of 3.5 GHz

After some optimization of the system, it was decided that a new VCO with better sensitivity was more desirable. This was ordered from Watkins-Johnson Company with a slight compromise in center-frequency as shown in Fig. 3-9. The center frequency is now 3.4 GHz, and over the tuning range of 3.15 to 3.65 GHz, both good sensitivity and linearity are obtained. For a 50-MHz deviation, a peak-to-peak voltage swing of 4 V is required. This corresponds to a drive power of only 40 mW, which is readily obtainable from wideband UHF amplifiers.

### 3.5 THE WIDEBAND FM DISCRIMINATOR

For the demodulation of analog signals, a wideband FM discriminator is required. The desired characteristics of the FM discriminator are as follows:

- Good linearity over a frequency range of 3- to 4-GHz and ability to handle modulation frequencies up to 400 MHz
- High sensitivity to input frequency variation and low sensitivity to input amplitude variations
- Output level high enough that the noise in the succeeding 400-MHz wideband amplifier does not appreciably degrade the signal-to-noise ratio established in the photodetector

Such a device has been fabricated at the beginning of this year. The design of this wideband discriminator is based on the work of Kincheloe and Wilkens (Refs. 4 and 5), who suggested the use of a microwave power divider and a 3-dB hybrid coupler connected by constant impedance transmission lines, as shown in Fig. 3-10a. The arrangement is a microwave analog of a one-dimensional optical interferometer; its action may be understood by considering the following.

The input signal to the discriminator,  $e_1 = A \cos 2\pi f t$ , is divided into two equal components, one of which passes through an additional propagation delay of  $\tau = 1/(2f_{sc})$ , where  $f_{sc}$  is the center frequency of the discriminator. Upon recombination in the 3-dB hybrid, the signal voltage  $e_a$  at the upper output port under matched (no reflection) conditions is given by

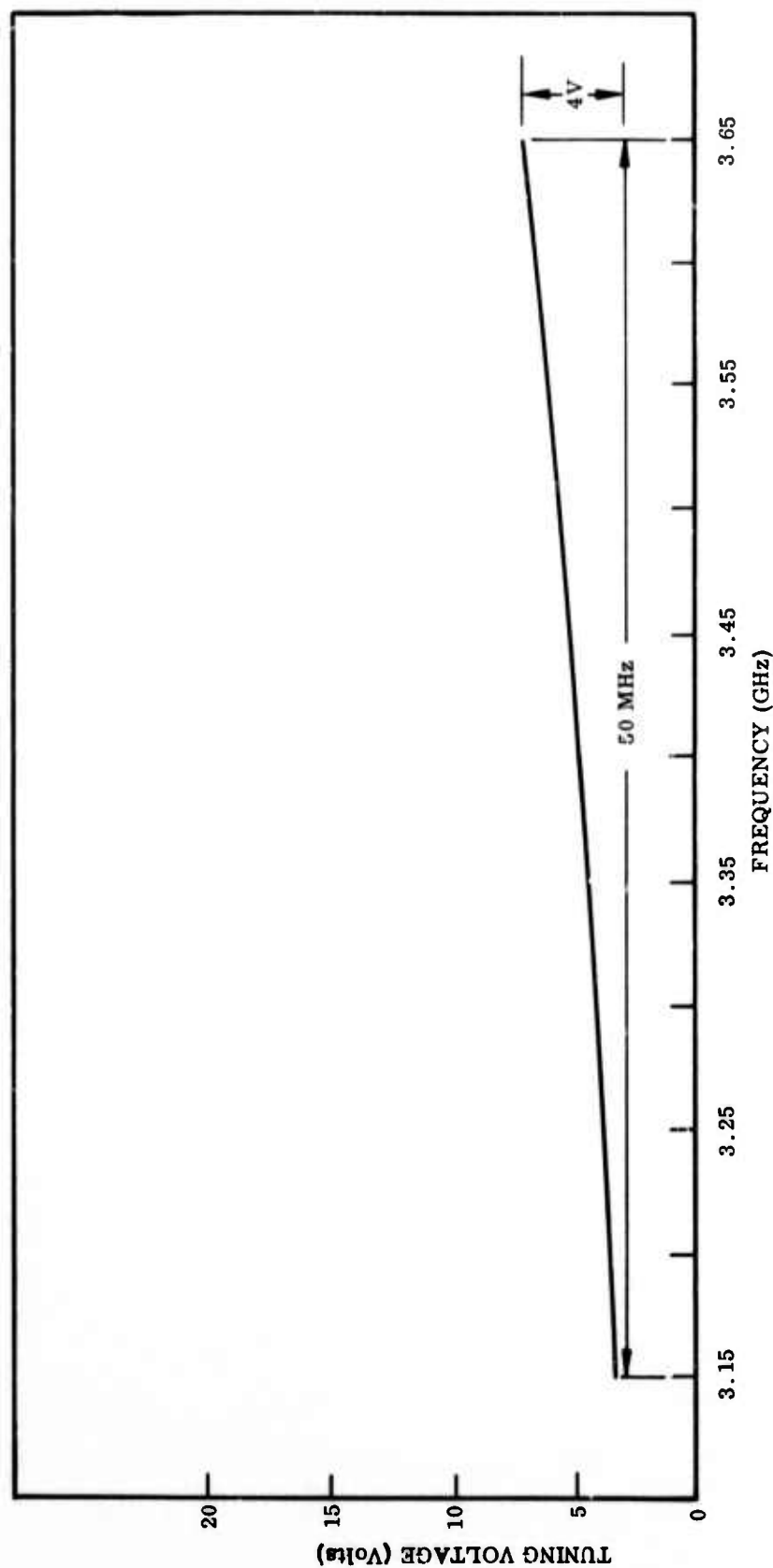


Fig. 3-9 Static Tuning Characteristics of the Second Voltage-Controlled Oscillator, With Center Frequency of 3.4 GHz

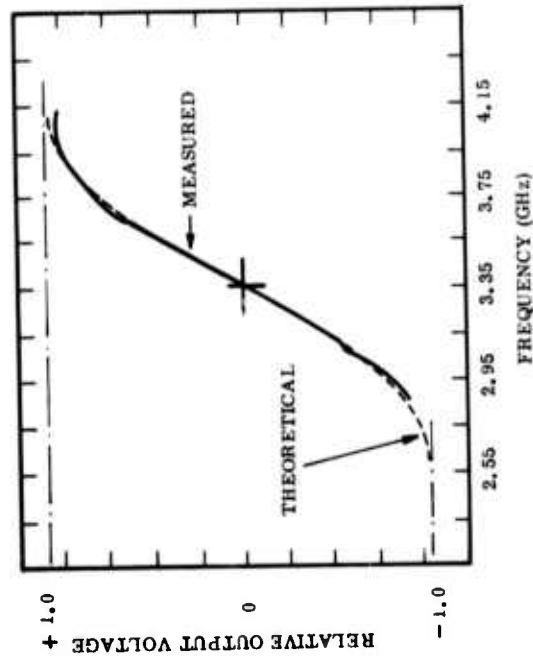
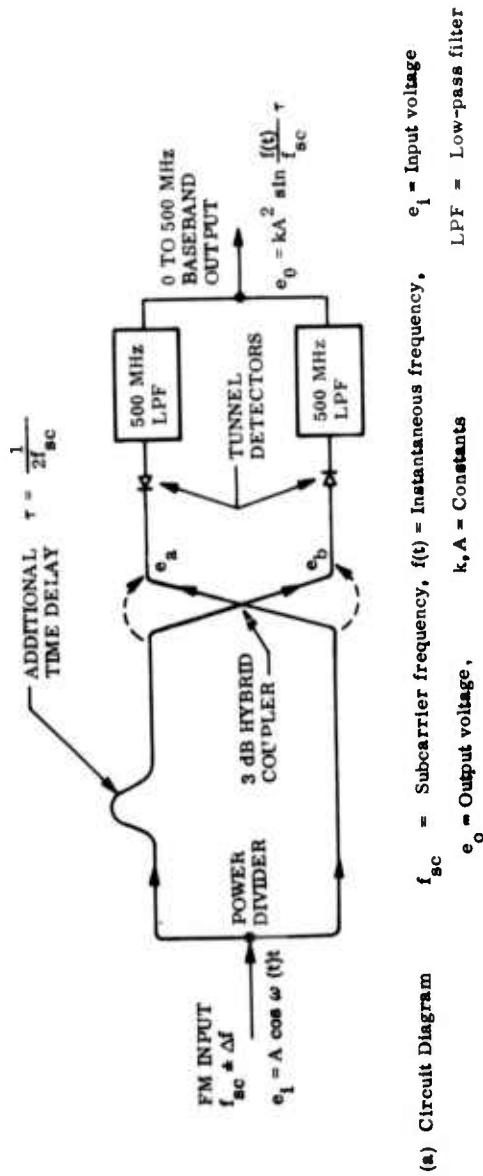


Fig. 3-10 The Wideband FM Discriminator

$$e_a = \frac{1}{2} A \cos (2\pi ft) + \frac{1}{2} A \cos (2\pi ft - 2\pi f\tau + \pi/2) \quad (3.1)$$

The first term is the result of the direct path (solid lines) through the coupler, and the second term is the result of the coupled path (dashed arrow). The added phase of  $\pi/2$  in the second term accounts for a constant difference in phase (independent of frequency) between the direct and coupled paths through the coupler. Similarly, the voltage  $e_b$  at the lower output port is

$$e_b = \frac{1}{2} A \cos (2\pi ft - 2\pi f\tau) + \frac{1}{2} A \cos (2\pi ft + \pi/2) \quad (3.2)$$

The voltages  $e_a$  and  $e_b$  are individually square-law detected, filtered through 500-MHz low-pass filters, and then recombined to give the recovered baseband signal. The detectors are arranged differentially so that the discriminator output is given by

$$e_o = k \left[ (e_a)^2 - (e_b)^2 \right] = kA^2 \sin(\pi f/f_{sc}) \quad (3.3)$$

where  $k$  is a constant, accounting for circuit losses including output loading and detector efficiency.

Linearity tests of this FM discriminator have been performed by slowly sweeping a constant-amplitude input signal from 3 to 4 GHz. The resulting discriminator output voltage is as shown in Fig. 3-10b along with the theoretically expected result of Eq. (3.3) plotted for  $KA^2$  normalized to unity.

From this curve, it is clear that good linearity is obtainable at 3.35-GHz subcarrier frequency, especially over deviations of under 250 MHz. Thus, the discriminator is useful over a wide frequency range.

### 3.6 SYSTEM IMPLEMENTATION

The system layout is essentially a hardware copy of the block diagrams shown in Figs. 2-2 through 2-5. Judicious choice of amplifiers and attenuators has to be determined to ensure proper signal levels so that signal-to-noise ratios are maximized and cross-talks are minimized.

Figure 3-11 shows the transmitter end of the laboratory system transmitting 2-Gbits/sec digital data. The components found in the lower and upper shelves are identified below.

On the lower shelf, the optical components in this system are shown. These consist of:

- A single-frequency laser (a commercial ion laser is shown used, to facilitate initial alignments and tests)
- A polarizer, which sets the light polarization at the desired 45-deg angle to the optical compensator and modulator crystal axes
- A servo-motor-driven optical compensator, which automatically sets the optical bias for the modulator
- A focusing lens, which places the optical beam waist at the center of the modulator crystal
- The electrooptical modulator
- An optical bias control unit, which senses the static optical bias condition of the modulator and produces an error signal to drive the compensator to quarter-wave optical-bias
- An output polarizer which converts optical polarization modulation into intensity modulation

An optical spectrum analyser is shown in Fig. 3-11, but this is used only for monitoring purposes.

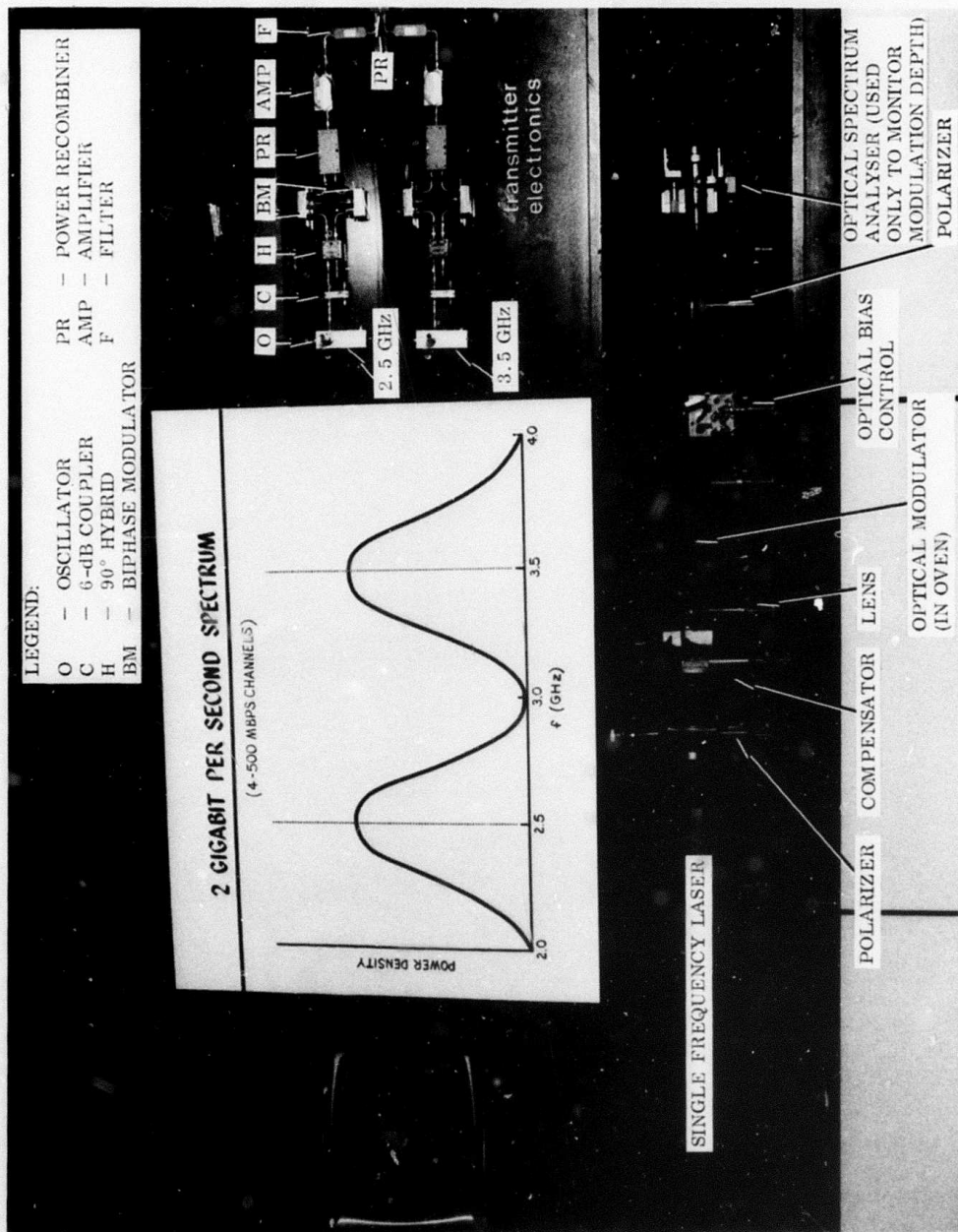


Fig. 3-11 Transmitter of 2-Gbits/sec Laboratory Optical Communication System



On the upper shelf, the transmitter electronics are shown. Components for the two subbands – one derives its subcarrier signal from a 2.5-GHz oscillator and the other from a 3.5-GHz oscillator – are clearly shown. Each subband includes identical types of components consistent with the frequency band. For instance, in the 2- to 3-GHz subband, power from the 2.5-GHz oscillator passes through a 6-dB coupler, with the main output directed to the receiver as the phase reference signal. The -6 dB output passes through a 90-deg hybrid to provide the "in-phase" and the "in-quadrature" channels. Each channel is then biphase-modulated at 500 Mbits/sec by the biphase modulator. The two channels are recombined in the power recombiner, amplified, and filtered to give a QPSK-modulated 2.5-GHz output. This is combined with the QPSK-modulated 3.5-GHz output to give a composite signal containing 2-Gbits/sec total data in a dual QPSK modulation format.

An illustration of the spectrum of the QPSK-modulated 2-Gbits/sec data, using two subcarriers as is done here, is shown in the center of Fig. 3-11. It should again be emphasized here that if PR generators at higher data rates (e.g., 1 Gbit/sec) were readily available, the entire 2-Gbits/sec data transmission could have been achieved using only one subcarrier (e.g., 3 GHz). The reasons for using two subcarriers are:

- (1) To make up the desired 2-Gbits/sec data rate in the most convenient way
- (2) To show that different data streams can be modulated onto different subcarriers which can then be multiplexed in the transmitter electronics and demultiplexed in the receiver electronics

Figure 3-12 shows the receiver end of the laboratory system. The optical system is again on the lower shelf, consisting simply of an optical attenuator, a focusing lens, and a photodetector (a static cross-field multiplier tube – CFPMT – is shown). A different CFPMT from the one purchased under this contract was used in these measurements because this tube did not appear to have the objectionable resonance at 2.5 GHz. From the CFPMT, the detected microwave signal is directed to the receiver electronics, shown in the upper shelf. The signal is divided into two halves in the 3-dB coupler; each half is used for the demodulation of digital data in one subband. Again,

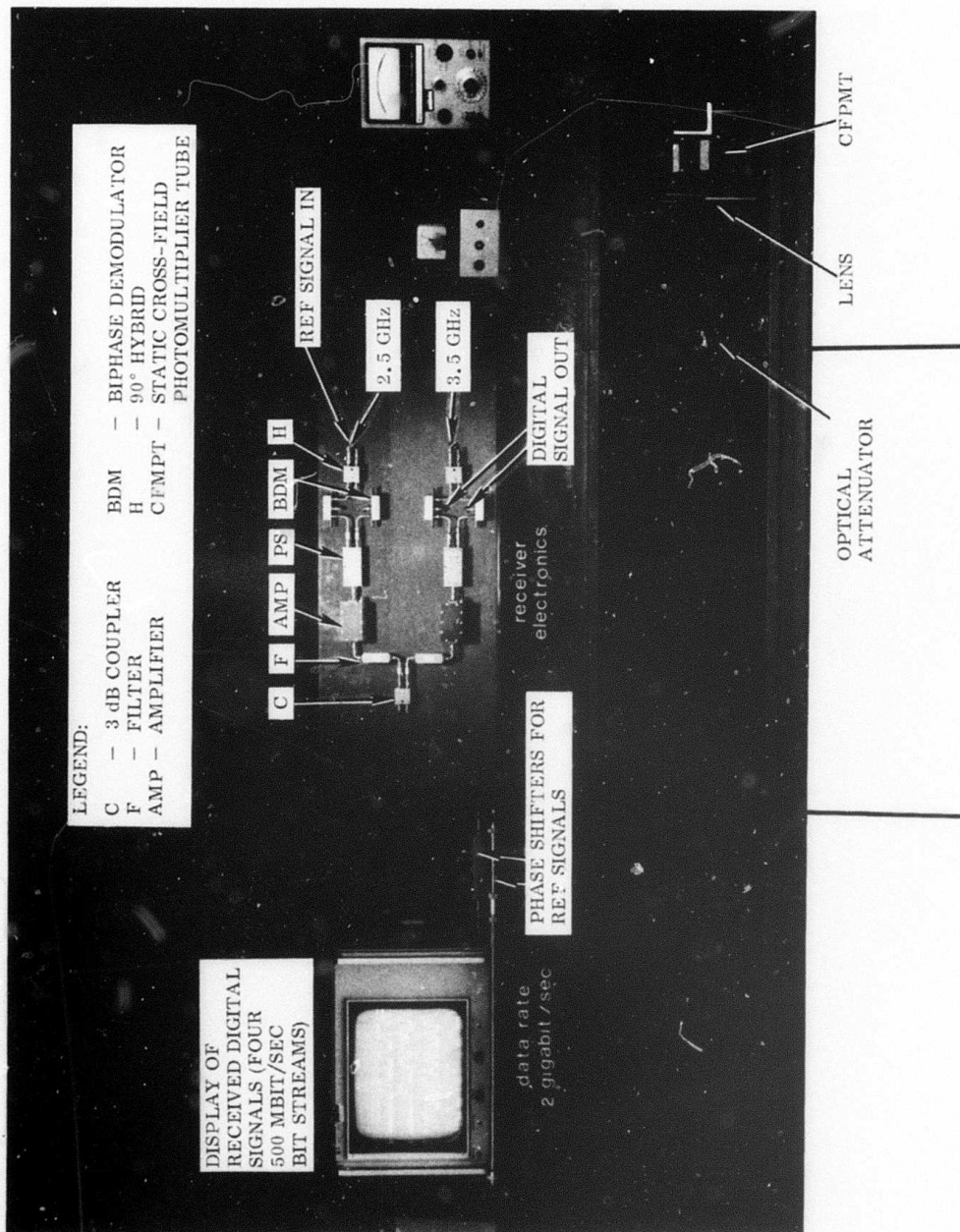


Fig. 3-12 Receiver of 2-Gbits/sec Laboratory Optical Communication System

the microwave components used for both subbands are identical in type, the only difference being in the frequency response. For instance, for the lower subband, the signal is filtered to give the 2- to 3-GHz components and amplified. This is then again divided into two halves, each half becoming the input signal for a biphas demodulator (BDM). The phase reference signal for a given subband comes from the 6-dB coupler in the transmitter, and is passed through a precision phase-shifter. At the BDM, therefore, the reference signal has a precise phase relationship to the input signal to effect proper demodulation. The reference signal is split by a 90-deg hybrid into an "in-phase" and an "in-quadrature" component; each component is directed to a BDM for the demodulation of a channel as explained in subsection 3.3. As a result, four streams of 500-Mbits/sec data, identical to the outputs from the word generators, are obtained. These are shown displayed on the sampling oscilloscope on the upper shelf.

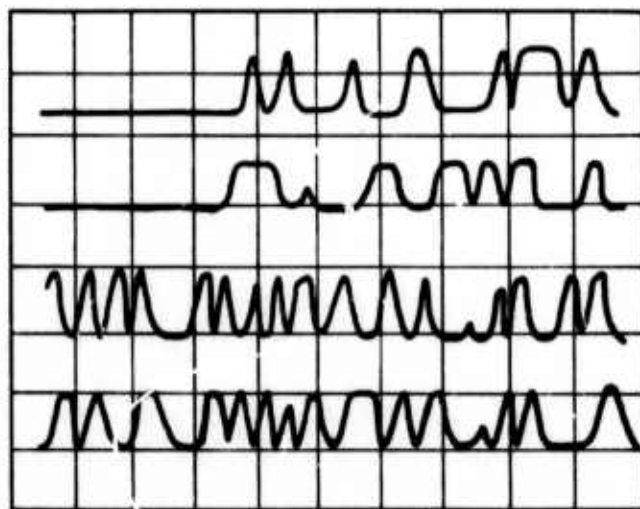
## Section 4

### SYSTEM TESTS

Experimental results of critical components such as the optical modulator, the VCO, etc., have been discussed in the earlier sections where appropriate. Only the system test results will be discussed in this section.

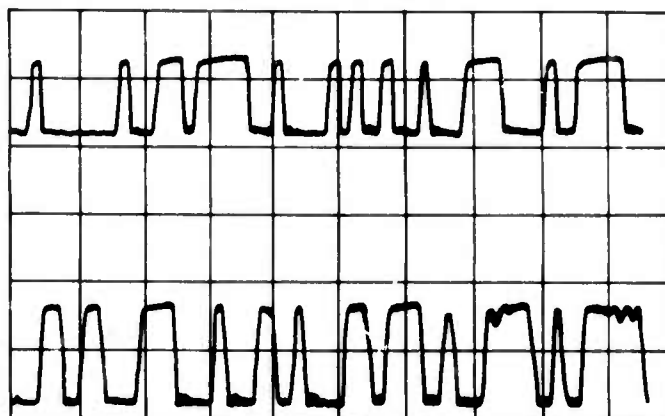
#### 4.1 QPSK DIGITAL MODULATION RESULTS

Figures 4-1, 4-2, and 4-3 show the typical results of the 2-Gbits/sec laboratory laser communication demonstration. Figure 4-1 is a sampling scope display of the 2-Gbits/sec data received via the laser link. A total of four 500-Mbits/sec channels are displayed: two of the channels are transmitted through the 2.5-GHz subcarrier, and two are transmitted through the 3.5-GHz subcarrier. All channels show good recovered signals.

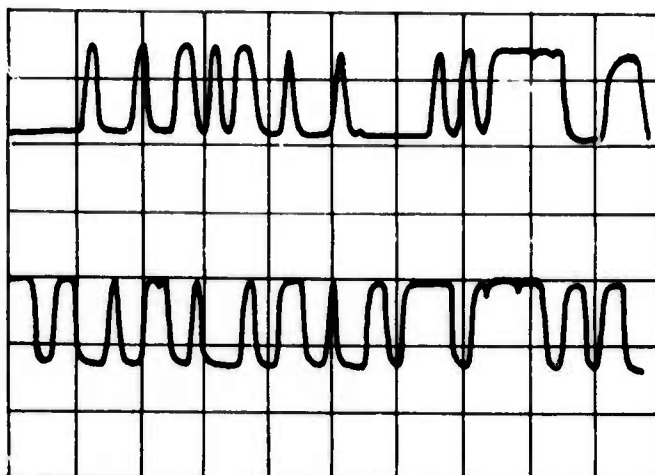


Upper Two Traces: 500 Mbits/sec each on 2.5-GHz subcarrier  
Lower Two Traces: 500 Mbits/sec each on 3.5-GHz subcarrier

Fig. 4-1 Sampling Scope Display of Four 500-Mbits/sec Streams Transmitted Through the Laser Link

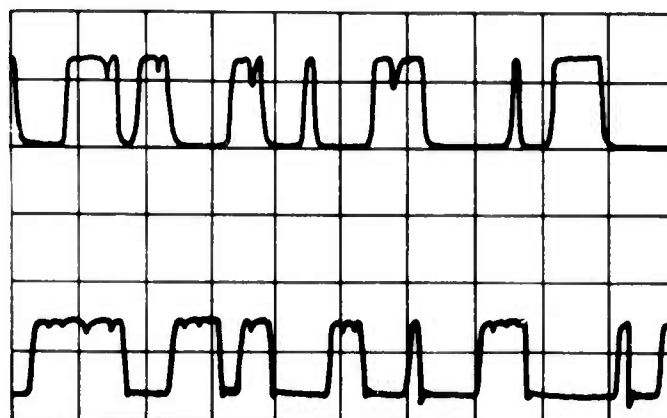


(a) Direct connection between transmitter and receiver electronics

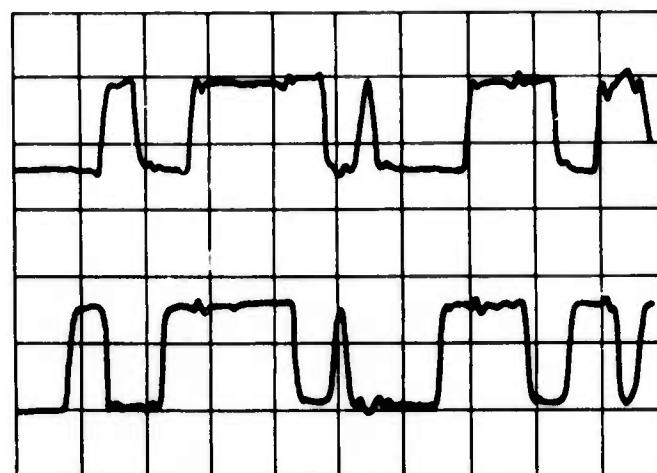


(b) As received through the laser link (TWT drive power 4 W: both 2.5-GHz and 3.5-GHz channels on)

Fig. 4-2 Waveforms of Two 500-Mbits/sec Streams on 2.5-GHz Subcarrier Frequency With Simultaneous 1-Gbit/sec Digital Signal on 3.5-GHz Subcarrier



(a) Direct connection between transmitter and receiver electronics



(b) As received through the laser link (TWT drive power 4 W: both 2.5-GHz and 3.5-GHz channels on)

Fig. 4-3 Waveforms of Two 500-Mbits/sec Streams on 3.5-GHz Subcarrier Frequency With Simultaneous 1-Gbit/sec Digital Signal on 2.5-GHz Subcarrier



Figures 4-2 and 4-3 show the degradation that takes place in the signals after being transmitted through the laser link. This includes the degradation due to the electro-optic modulator and the photodetector. Each figure is for the data over a particular subcarrier: the two top traces show the sampling scope display of the two 500-Mbits/sec data outputs which results from a direct connection (hardwire) from the traveling-wave tube amplifier, with suitable attenuation, to the microwave receiver. The bottom two traces show the two 500-Mbits/sec outputs which result from the transmission over the laser link. These tests were run using a commercial argon ion laser, operating single-mode, single-frequency at  $\lambda_0 = 0.5145 \mu\text{m}$ . The visible wavelength, rather than  $1.06 \mu\text{m}$ , was used for these initial tests because of the ease of optical alignment and better photodetector response.

The traces in Figs. 4-2 and 4-3 show that there is not a one-to-one correspondence between the data bits in the upper traces and those in the lower traces, because the amount of delay in the laser transmission and reception causes a different portion of the PR signal to appear on the oscilloscope, and no provision has been made in these experiments to compensate for this difference in delay. The important aspect of these data is to show the degree to which the character of the data waveform is degraded. From these traces, it is clear that the rise and fall times are lengthened and the corners rounded. However, it is also clear that the bits are still readily recognizable as ones or zeroes even to the eye, although those in Fig. 4-3 appear to be noisier. This noisy performance arises from the fact that the traveling-wave tube used has relatively lower gain at the high-frequency end, and that the cross-field photomultiplier tube (CFPMT), which also has a lower response at the high-frequency end, is used in these measurements. It is estimated that by using matched-filter detection, the data should be recovered with 2- to 3-dB degradation in performance from the theoretical integrate-and-dump performance.

The performance for the 2-Gbits/sec transmission shown above is considered good for this feasibility demonstration since it shows that the system does have the designed bandwidth of 2 GHz and will accept the desired high data rate. Thus, no additional tests will be run using the 2-Gbits/sec data. Instead, efforts will all be concentrated on the

1-Gbit/sec digital and 1-GHz analog modulation experiment, which is the main experiment to be performed under this contract.

#### 4.2 FM-ANALOG MODULATION RESULTS

Tests for the transmission of the 1-Gbit/sec digital and 1-GHz analog data have also been initiated in the laboratory using the visible laser. The 3.5-GHz subcarrier was used for the analog signals and the 2.5-GHz subcarrier was used for the digital signals. (The use of these subbands is different from that shown in Fig. 2-4. This will become clear in the latter paragraphs of this section.) No difficulty with the digital signals was encountered since the subsystem had been well "debugged" in the earlier experiments. However, some difficulty has been experienced with the 1-GHz analog subsystem as detailed in the following paragraphs.

The first voltage-controlled oscillator (VCO) used for the FM transmission of the analog signals required rather high driving voltages (see Fig. 3-8 and discussions in Section 3). To provide these high voltages in a 50- $\Omega$  system, high drive power is required. This forces the driver amplifier to operate in saturation, thereby causing intermodulation between the various analog signals (local TV channels, 4, 5, 7, and 9). In addition, because of the power limitation of the driver amplifier, the FM deviation was rather low so that the received signal-to-noise ratio (S/N) was high. After much effort had been expended in designing frequency filters (traps) and inserting various attenuators and amplifiers to reduce intermodulation, the results were still considered unsatisfactory.

A second VCO was then ordered. This VCO required much less driving power for its operation so that good linearity with reasonable deviation could be obtained. The unit has been delivered, and work is now in progress in the system tests. Results to date showed that intermodulation has been greatly reduced. However, the S/N ratios for the received signals are still rather poor, typically in the 20-dB range. (For good TV picture reception, a S/N ratio in the range of 40 to 45 dB is required.)

The causes for such a low S/N performance are attributed to.

- (1) The frequency deviation is still small ( $\sim 35$  MHz at a carrier frequency of 3.5 GHz) so that there is only a small amount of signal content in the FM subsystem.
- (2) The allowable optical power on the photocathode is limited ( $\sim 5 \mu\text{W}$ ) and the high-frequency response of the CFPMT is poor, causing further reduction of the signal content with respect to system noise.

Consideration is now seriously being given to using the lower subband (2.5-GHz subcarrier) for FM analog transmission and the upper subband (3.5-GHz subcarrier) for digital transmission as shown in Fig. 2-4. This change in direction is based on the following facts:

- (1) High power (several watts), wideband (dc to 500 MHz) baseband amplifiers are not commercially available. Thus, to minimize intermodulation, frequency deviation has to be kept small; i. e., the signal content is kept small.
- (2) The performance of the CFPMT is poorer than expected in the high-frequency end of the band.
- (3) In the lower subband, the traveling-wave tube, the photodetectors all have good response so that higher S/N is obtainable.
- (4) For the transmission of digital signals, an S/N ratio of 20 dB gives a good signal display, while for the transmission of analog signals, a minimum S/N of 30 dB is required.

Section 5  
CONCLUSIONS AND FUTURE PLANS

During the first six months, all essential components for the system demonstration have been obtained. They all appear to work well, although specific improvements for any one component are always welcome. Feasibility demonstration of the 2-Gbits/sec data transmission has been demonstrated. The degradation in received signal over a laser beam is only slight as compared with that received over a cable. In general, it is estimated that the received signal over a laser beam can be recovered with a 2- to 3-dB degradation in performance from the theoretical integrate-and-dump performance.

Experimental transmission of 1-Gbit/sec digital and 1-GHz analog data has been attempted and is still in progress. The results so far have not been very good; typical S/N ratios of 20 dB are obtained for the analog signals. The problems encountered have all been of practical nature; e.g., the voltage-controlled oscillator requires high drive power, poor frequency response of the phototube, etc. It is believed that by applying additional efforts in adjusting the system parameters, most of the problems can be alleviated.

For the remaining period of this contract, continuing effort will be applied to the FM-analog subsystem. In particular, the use of different photodetectors will be studied, and the interchange of subbands for analog and digital transmission will be investigated.

Section 6  
REFERENCES

1. R. C. Ohlmann, W. Culshaw, K. K. Chow, H. V. Hance, W. B. Leonard, and J. Kannelaud, High-Efficiency, Single-Frequency Laser and Modulator Study, First Annual Technical Report, 30 Sep 1971, Contract No. N00014-71-C-0049, Office of Naval Research/Advanced Research Project Agency
2. -----, High-Efficiency, Single-Frequency Laser and Modulator Study, Second Annual Technical Report, 31 Dec 1972, Contract No. N00014-71-C-0049, Office of Naval Research/Advanced Research Project Agency
3. R. B. Ward and D. G. Peterson, Design Performance Verification I, Technical Report AFAL-TR-73-371, Nov 1973, Air Force Avionics Laboratory, Wright-Patterson Air Force Base, Ohio
4. W. R. Kincheloe and M. W. Wilkens, "Phase and Instantaneous Frequency Discriminators," U.S. Patent 3,395,346, Jul 30, 1968
5. M. W. Wilkens and W. R. Kincheloe, Microwave Realization of Broadband Phase and Frequency Discriminators, Stanford Electronics Laboratory, Tech. Rep., 1962/1966-2, Nov 1968, DDC ASTIA Doc. AD 849,757